

High-Fidelity Numerical Simulations of Multiphysics Turbulent Flows in Complex Geometries

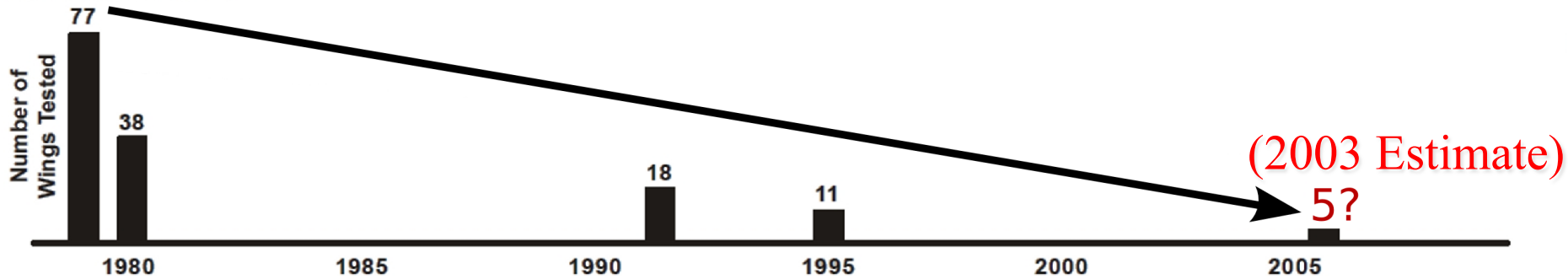
Parviz Moin
Center for Turbulence Research
August, 2012



A Story from the aircraft industry



1980 state of the art

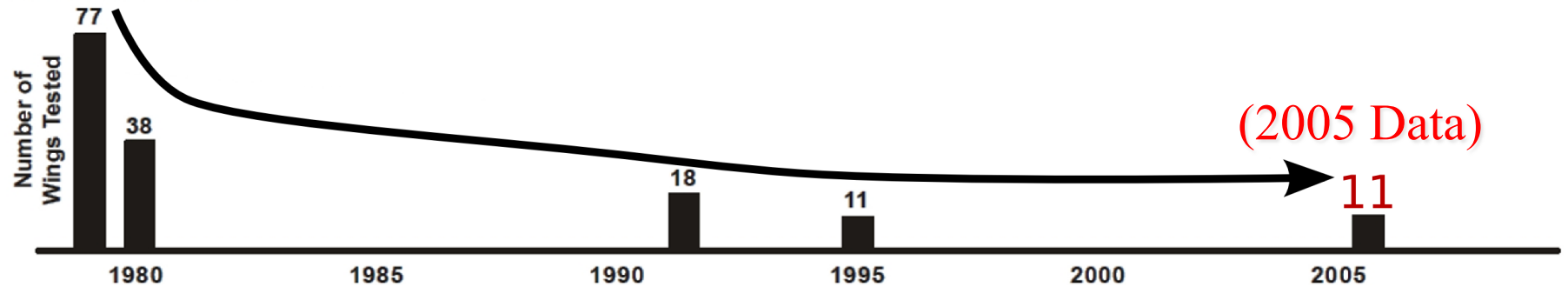


- In 2003, Boeing estimated that the number of wing tests for 787 would be 5, representing a significant reduction from 11 a decade earlier.
- Estimates were based in large part on the increased use of simulation and enormous increase in compute resources during the decade 1995 to 2005 (~1000x)

A Story from the aircraft industry



1980 state of the art



- By 2005, the actual number of wing tests required was 11, the same as a decade earlier
- **Why?** computer power was not the largest source of uncertainty in their predictions: it was **model fidelity**.
- High fidelity methods that incorporate more “first principles” are a path to predictive simulations because they can leverage the dramatic increase in compute power available

Multi-physics Turbulent Flows Modeling Challenges

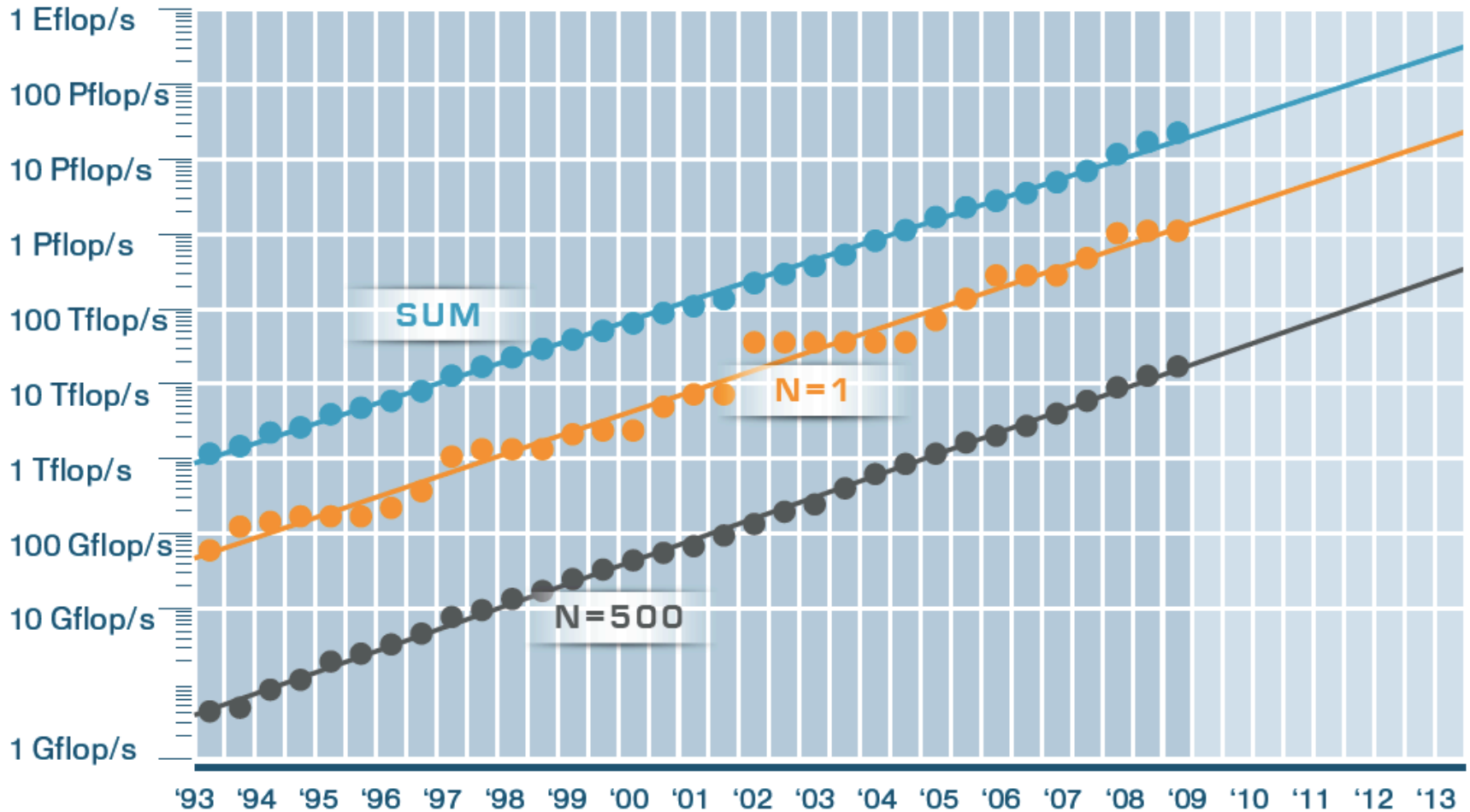
Many modeling and simulation challenges can benefit from a high-fidelity approach:

- Compressible flow with shocks and complex mixing
- Laminar/turbulent flow transition
- Chemical kinetics and reacting flows
- Two Phase flow
- Combustion dynamics and coupled thermoacoustics
- Integrated system issues, e.g. combustor/Turbine

Goal for this talk is to illustrate where we are in many of these areas, and where we are going in the next 10 years

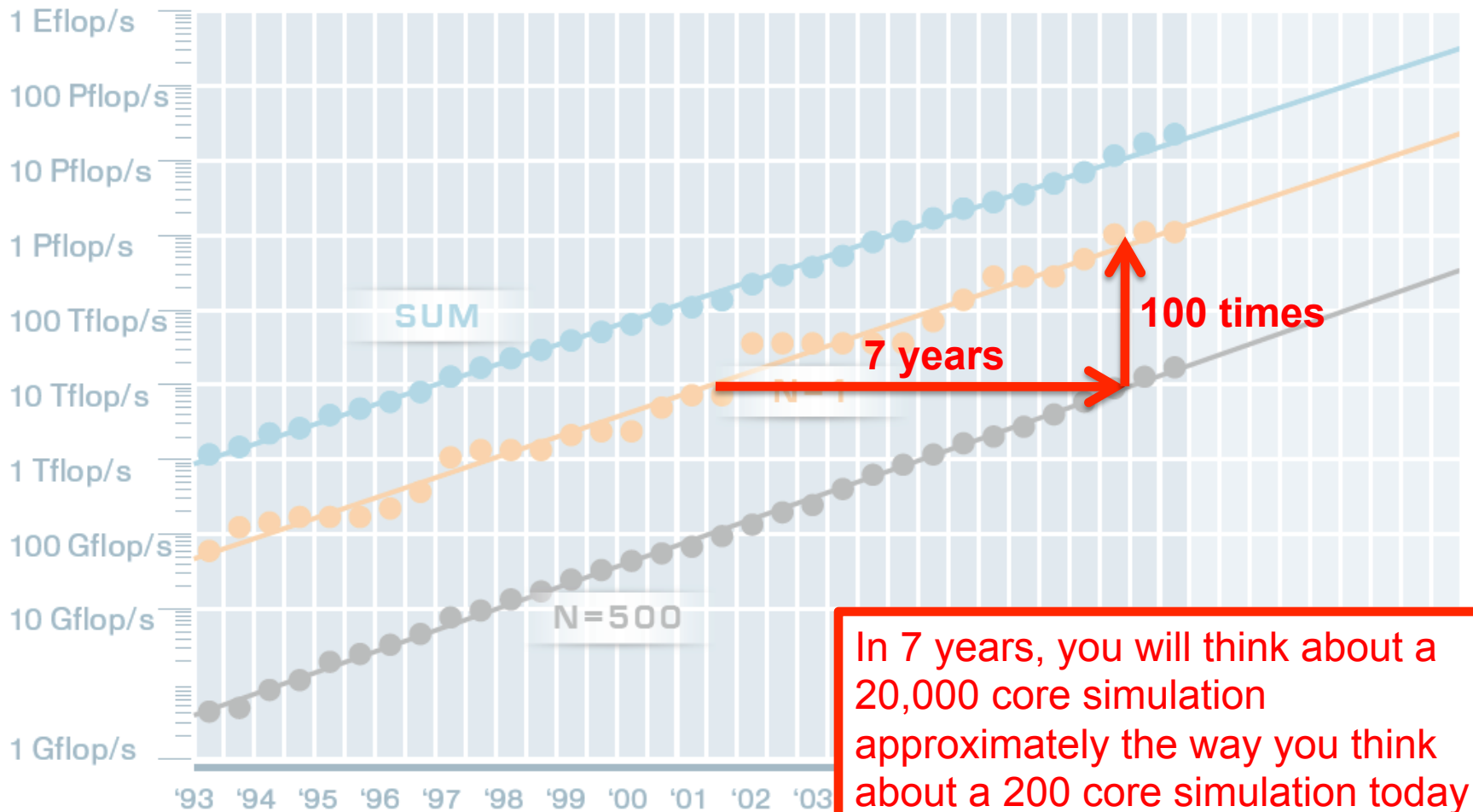
Supercomputer Hardware trajectory

Growth in supercomputing power:
Top 500 list, www.top500.org



How to think about 20K processors:

Growth in supercomputing power:
Top 500 list, www.top500.org



Computer systems

Rank	Site	Computer/Year Vendor	Cores	R _{max}	R _{peak}	Power
1	RIKEN Advanced Institute for Computational Science (AICS) Japan	K computer, SPARC64 VIIIfx 2.0GHz, Tofu interconnect / 2011 Fujitsu	705024	10510.00	11280.38	12659.9
2	National Supercomputing Center in Tianjin China	NUDT YH MPP, Xeon X5670 6C 2.93 GHz, NVIDIA 2050 / 2010 NUDT	186368	2566.00	4701.00	4040.0
3	DOE/SC/Oak Ridge National Laboratory United States	Cray XT5-HE Opteron 6-core 2.6 GHz / 2009 Cray Inc.	224162	1759.00	2331.00	6950.0
4	National Supercomputing Centre in Shenzhen (NSCS) China	Dawning TC3600 Blade System, Xeon X5650 6C 2.66GHz, Infiniband QDR, NVIDIA 2050 / 2010 Dawning	120640	1271.00	2984.30	2580.0
5	GSIC Center, Tokyo Institute of Technology Japan	HP ProLiant SL390s G7 Xeon 6C X5670, Nvidia GPU, Linux/Windows / 2010 NEC/HP	73278	1192.00	2287.63	1398.6
6	DOE/NNSA/LANL/SNL United States	Cray XE6, Opteron 6136 8C 2.40GHz, Custom / 2011 Cray Inc.	142272	1110.00	1365.81	3980.0
7	NASA/Ames Research Center/NAS United States	SGI Altix ICE 8200EX/8400EX, Xeon HT QC 3.0/Xeon 5570/5670 2.93 Ghz, Infiniband / 2011 SGI	111104	1088.00	1315.33	4102.0
8	DOE/SC/LBNL/NERSC United States	Cray XE6, Opteron 6172 12C 2.10GHz, Custom / 2010 Cray Inc.	153408	1054.00	1288.63	2910.0

kW

Power – and the Exaflop machine in 2020

- ❑ DOE planning to build an exaflop machine by 2020 that uses 20MW (dramatically reduced power/flop)
- ❑ However, scaling of our problems is hard: e.g. for a factor of 2 in grid length scale, we need a factor of $\sim 2^4=16$ in computation power, or about 4 years
- ❑ For a factor of 10 in length scale, need ~ 13 years

In the next decade:

- ❑ physics-based sub-grid modeling will remain a critical part of high-fidelity simulations
- ❑ Methods should carefully focus increased fidelity to beat these estimates (e.g. unstructured grids, fidelity of chemistry)

Elements of Large Eddy Simulation (LES)

Traditional components

- Filtering, commutation, constitutive equations
- Subgrid scale modeling
- Wall modeling
- Numerical Methods

New considerations

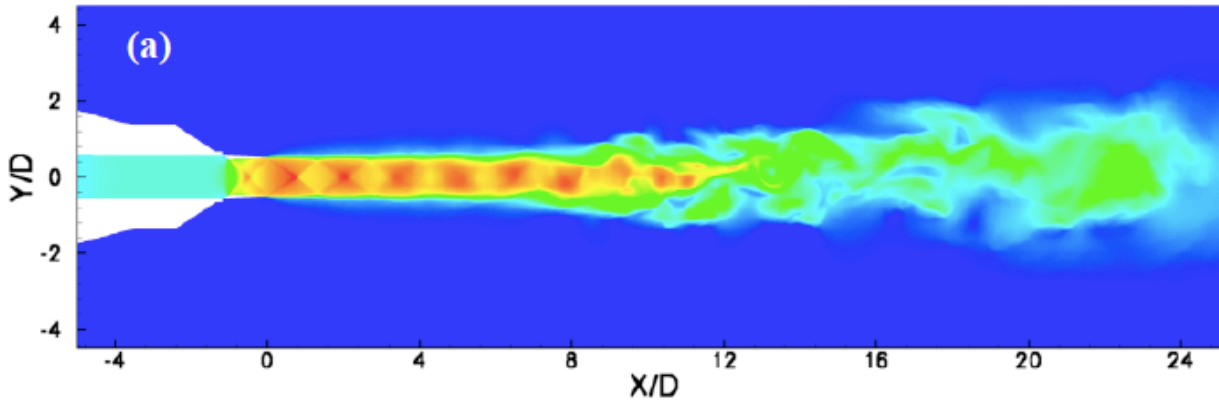
- Interlink among above components
- Computer science
- Multiphysics (Combustion, Multiphase...)

Stand-alone research in anyone of these areas is not going to have large engineering impact

Not all LES's are equal: Numerical Methods

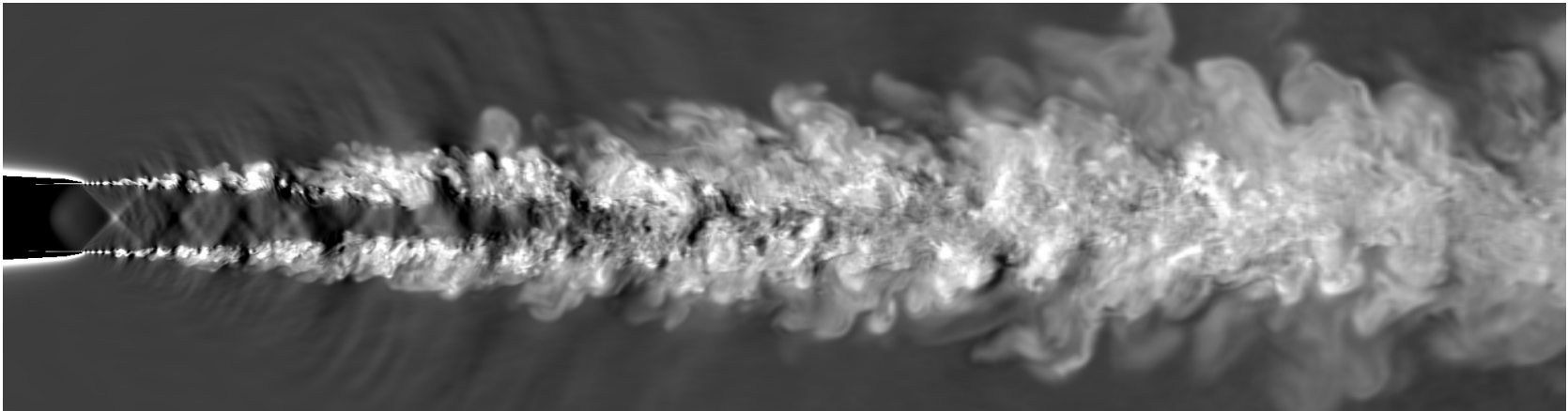
- It is important for LES calculations to predict accurately the quantities that led to choosing LES in the first place (e.g., turbulent fluctuations, acoustic sources, mixing,...).
- Numerical dissipation present in most codes, originally designed for RANS, is inadequate for LES
- Dispersion errors important for compressible flow and prediction of aerodynamic noise
- LES imposes additional requirements on mesh quality and size

Visual evidence of Numerical Dissipation in LES



From Liu et al.
AIAA J. 2009,
MILES

Supersonic Jet LES using MILES-base method



Supersonic Jet LES using low-dissipation method (Charles)

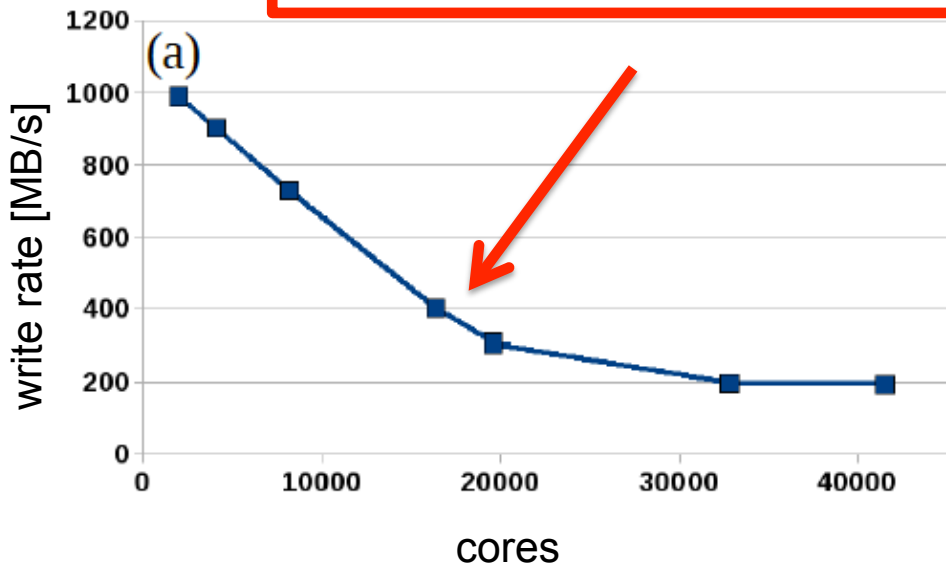
An example of a solver built specifically for LES: Charles

- ❑ Unstructured meshes, any elements including hanging nodes
- ❑ Novel low-dissipation/dispersion unstructured operators
- ❑ Massively Parallel and Scalable throughout (pre, solve, post, I/O)
- ❑ Multiple solvers based on a common infrastructure
- ❑ Multiphysics models (Liquid spray, combustion, shock capturing, acoustics)
- ❑ Highly customizable (e.g. different combustion models, ...)
- ❑ Dynamic Subgrid scale models

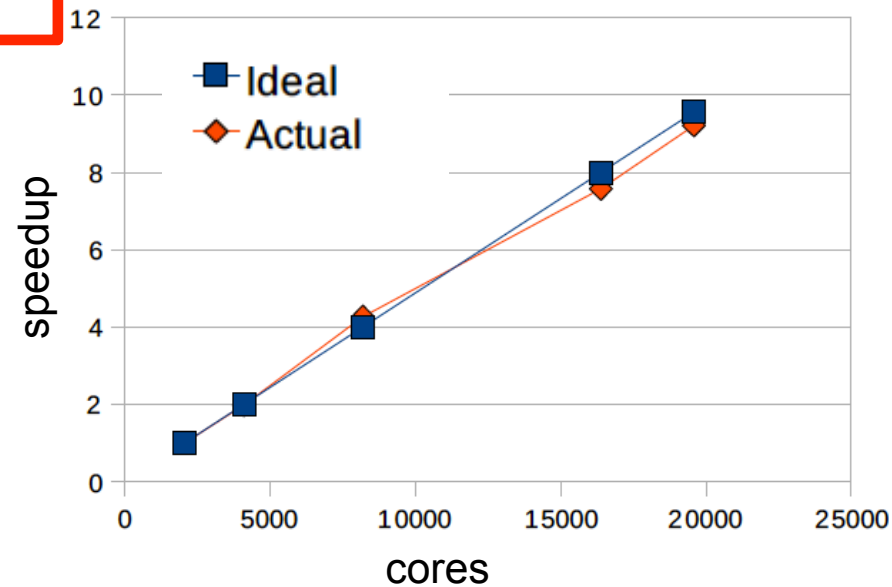
Massively Parallel Solver and I/O

- Special attention has been directed to code-scalability and parallel performance on today's massive supercomputing systems

Parallel, scalable I/O critical for efficiently building databases for subsequent interrogation with other parallel tools

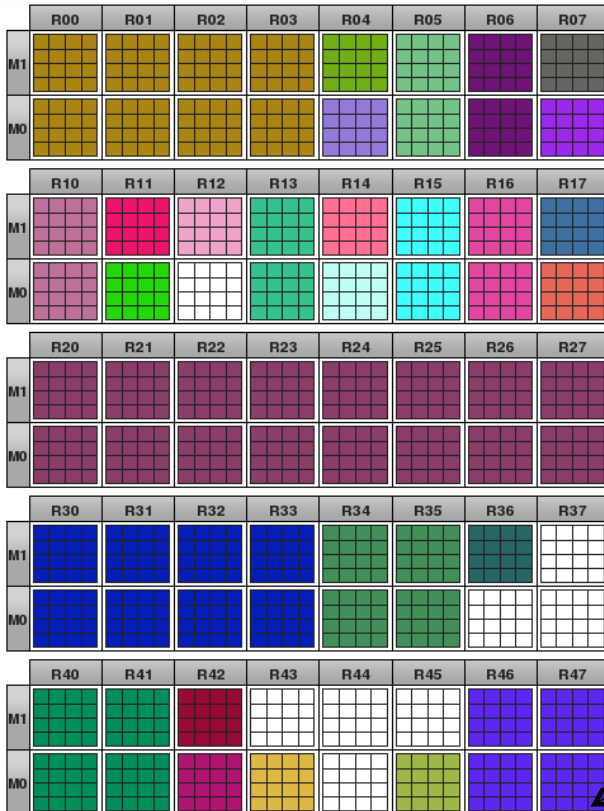
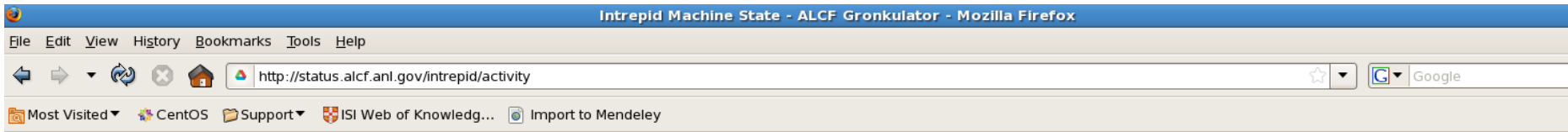


Measured write-rate (I/O)
Charles Jet Simulation on Cray



speedup/time,
Charles on Cray X6

One way to use a supercomputer



Running Jobs									
Running Jobs		Queued Jobs		Reservations					
Total Running Jobs: 28									
Job Id	Project	Run Time	Walltime	Location	Queue	Nodes	M		
452983	Turbulent_Mixing	11:17:37	12:00:00	ANL-R05-1024	prod-long	1024	dual		
451127	RT_Instability_In	10:50:25	12:00:00	ANL-R00-R03-4096	prod-long	4096	vn		
452984	Turbulent_Mixing	09:54:15	12:00:00	ANL-R10-1024	prod-long	1024	dual		
453190	Turbulent_Mixing	03:34:27	04:59:00	ANL-R06-1024	prod-short	1024	dual		
453261	LatticeQCD	03:17:02	06:00:00	ANL-R04-M0-512	backfill	512	scrip		
452776	LatticeQCD	00:53:45	01:30:00	ANL-R16-1024	backfill	1024	vn		
452817	LatticeQCD	00:52:53	01:45:00	ANL-R30-R33-4096	backfill	4096	vn		
452886	LatticeQCD	00:52:39	01:15:00	ANL-R34-R35-2048	backfill	2048	scrip		
452484	LatticeQCD	00:52:26	01:20:00	ANL-R20-R27-8192	backfill	8192	vn		
453333	LatticeQCD	00:48:27	02:45:00	ANL-R11-M1-512	backfill	512	scrip		
453347	SU_Climate	00:36:13	02:20:00	ANL-R11-M0-512	prod-short	512	scrip		
452746	LatticeQCD	00:33:39	01:15:00	ANL-R40-R41-2048	backfill	2048	scrip		
453119	LatticeQCD	00:33:02	01:00:00	ANL-R46-R47-2048	backfill	2048	vn		
453341	LatticeQCD	00:21:04	03:00:00	ANL-R07-M1-512	backfill	512	scrip		
453130	LatticeQCD	00:20:07	01:30:00	ANL-R17-M0-512	backfill	512	vn		
453353	SU_Climate	00:19:42	04:00:00	ANL-R04-M1-512	prod-short	512	scrip		
452317	Operations	00:18:44	00:45:00	ANL-R17-M1-512	diags	512	scrip		
453355	LatticeQCD	00:15:31	00:20:00	ANL-R36-M1-512	backfill	512	vn		
452355	Operations	00:15:04	00:45:00	ANL-R42-M1-512	diags	512	scrip		
453357	SU_Climate	00:12:41	00:40:00	ANL-R42-M0-512	prod-short	512	scrip		
453224	LatticeQCD	00:12:27	06:00:00	ANL-R07-M0-512	backfill	512	scrip		
453356	LatticeQCD	00:10:31	00:20:00	ANL-R43-M0-512	backfill	512	vn		
453321	LatticeQCD	00:08:41	00:20:00	ANL-R45-M0-512	backfill	512	vn		
452955	LatticeQCD	00:06:32	01:00:00	ANL-R15-1024	backfill	1024	scrip		
452311	Operations	00:06:09	00:45:00	ANL-R14-M1-512	diags	512	scrip		
452310	Operations	00:05:56	00:45:00	ANL-R14-M0-512	diags	512	scrip		
453					backfill	1024	scrip		
453					backfill	512	vn		

One square = 128 processors

Empty nodes are not idle; they are making room for the next queued job.

A better way to use a supercomputer

Grab File Edit Capture Window Help

Intrepid Machine State – ALCF Gronkulator

http://status.alcf.anl.gov/intrepid/activity

Running Jobs Queued Jobs Reservations

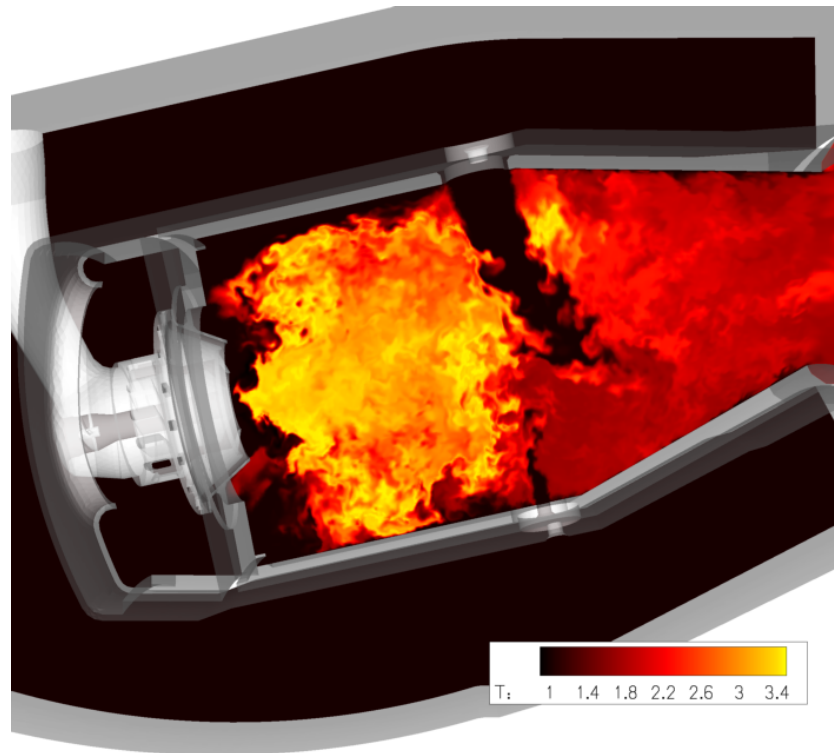
Total Running Jobs: 1

Job Id	Project	Run Time	Walltime	Location	Queue	Nodes	Mode
461574	SS_Jetnoise	00:01:13	23:45:00	ANL-R00-R47-40960	R.jet	40960	vn

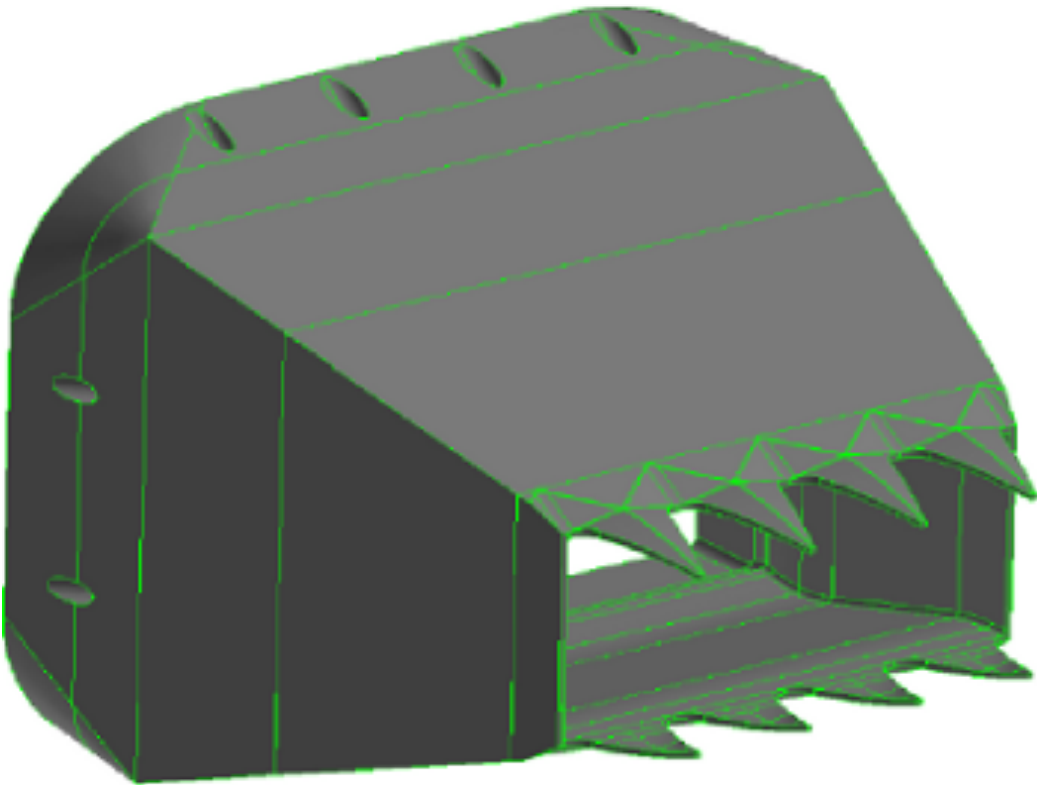
- Jet noise prediction
- 500M unstructured mesh
- 163,840 cores x 4 days = 16M core-hours
- 80% parallel efficiency – depended critically on load balancing shock-capturing faces

Decision to go unstructured

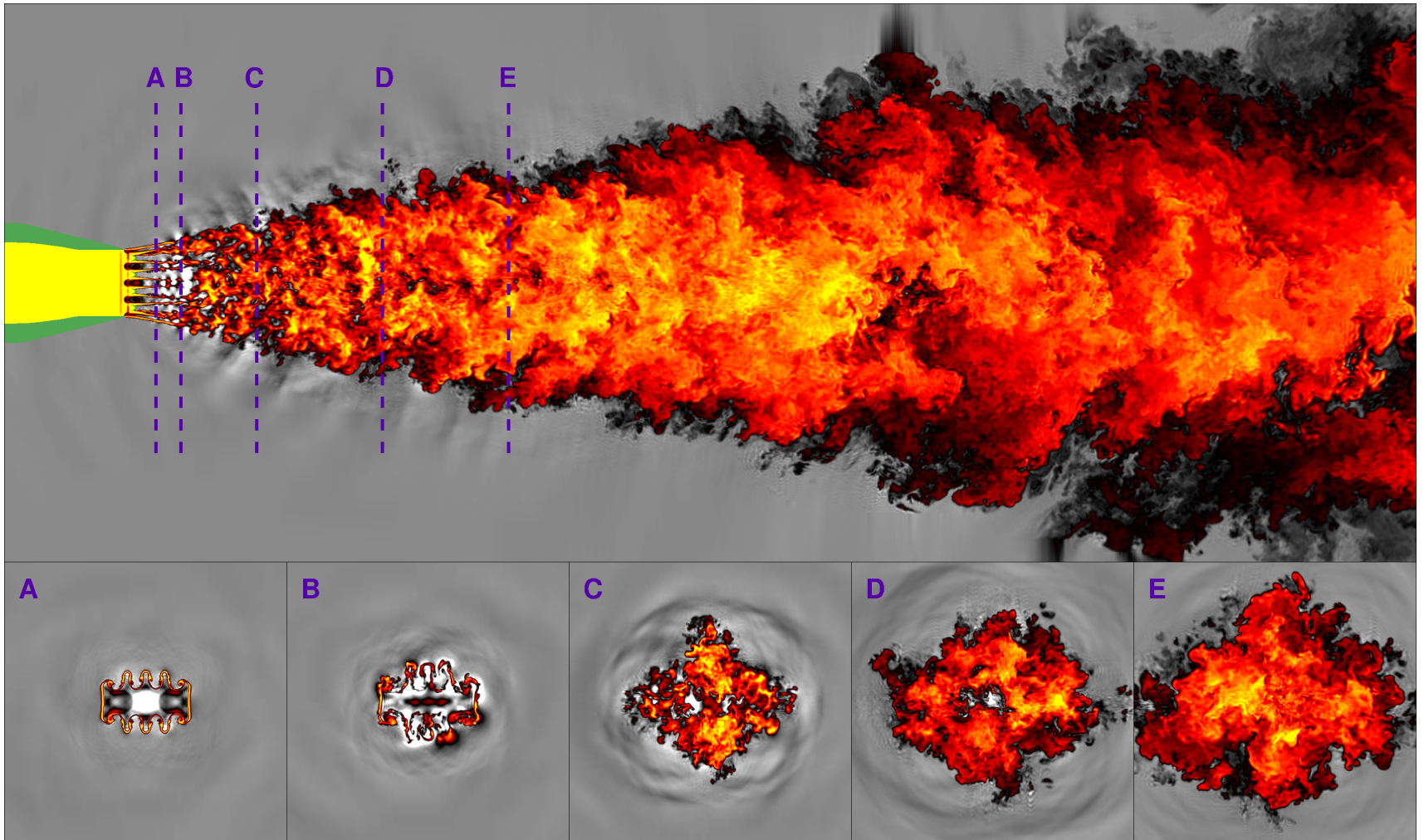
- ❑ Penalty on a per-node/cv basis (5x+), however:
- ❑ Complex geometry (e.g. combustor + turbine stage)
- ❑ Mesh Flexibility: adaptation and refinement
- ❑ Massive parallelism



Effect of Chevrons



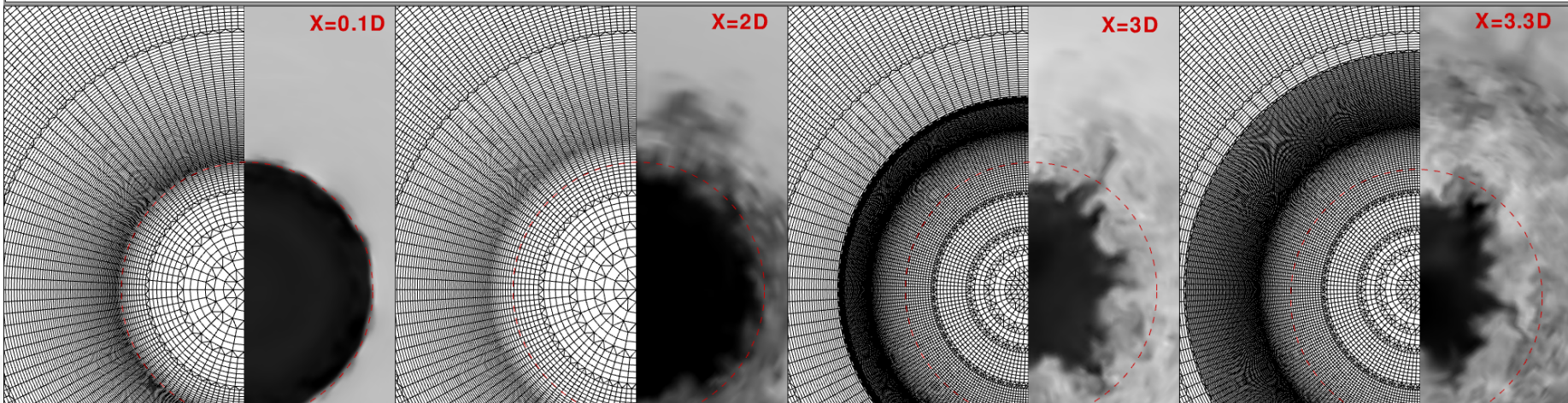
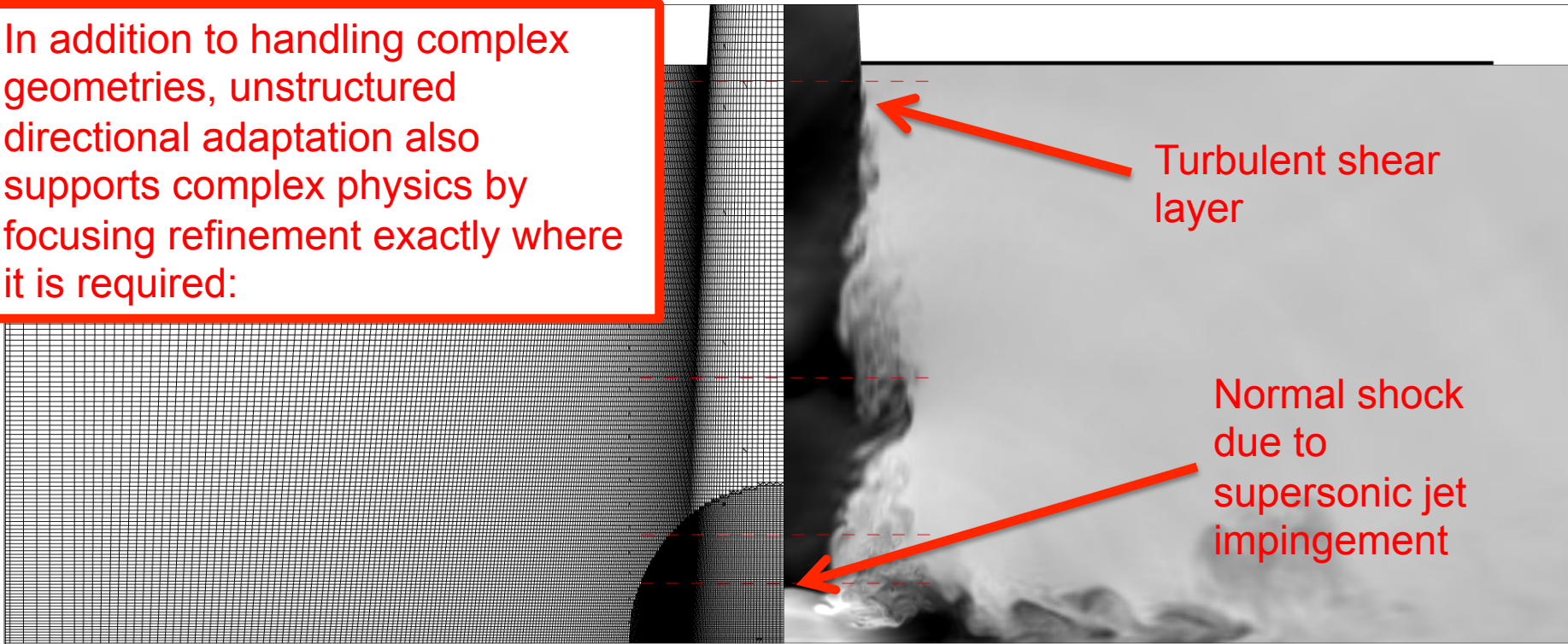
Some recent HPC experiences: Supersonic Jet Noise on Argonne Bluegene



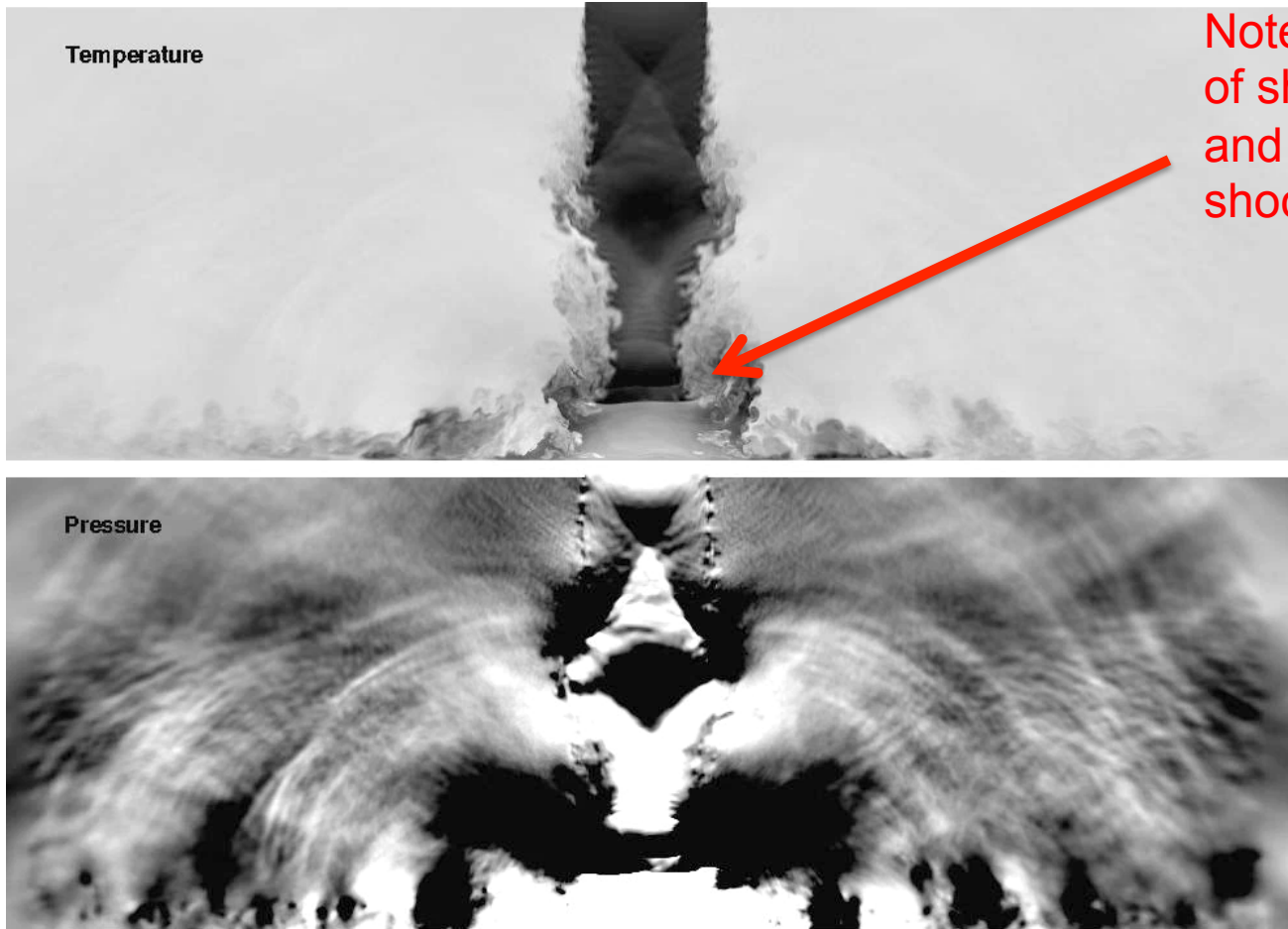
Instantaneous temperature field predicted from a heated rectangular jet with chevrons: simulations of J. Nichols

Directional-refinement capability in Charles

In addition to handling complex geometries, unstructured directional adaptation also supports complex physics by focusing refinement exactly where it is required:



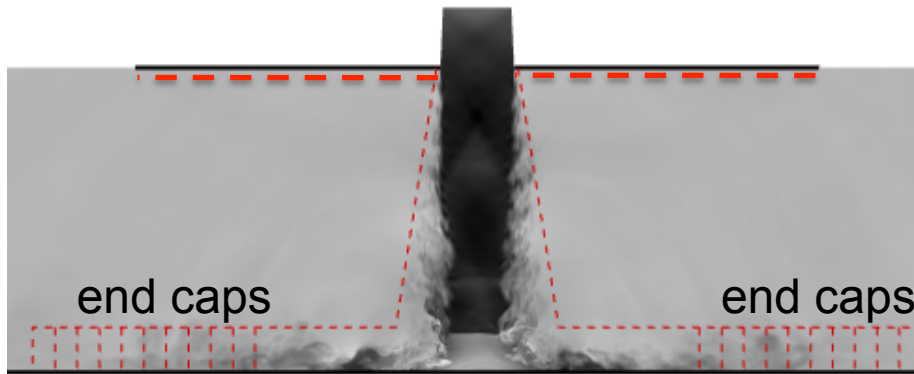
Flow physics of high speed jet impingement (ideally-expanded)



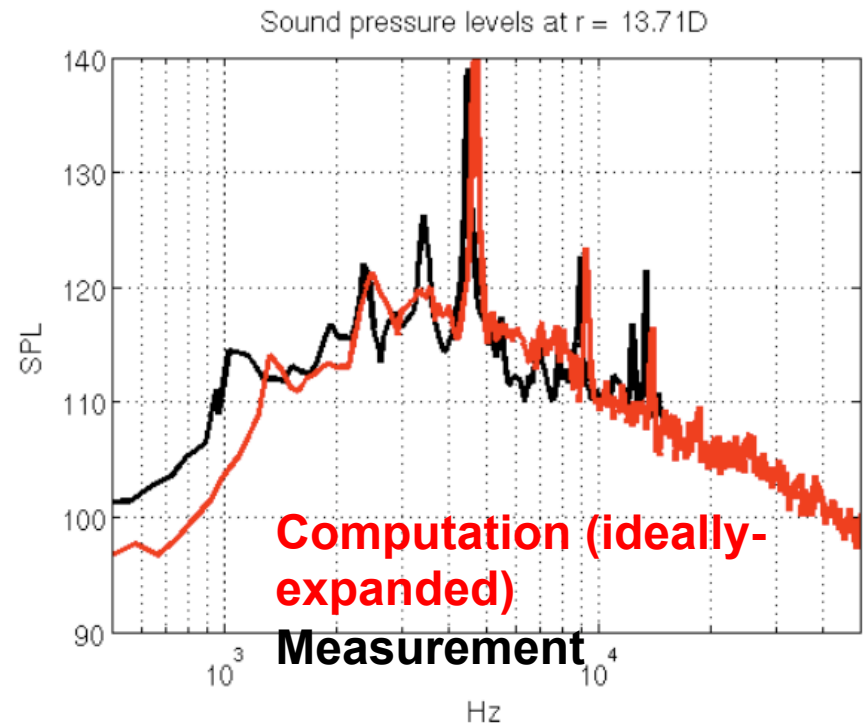
Note interaction
of shear layer
and normal
shock

Acoustic computations: a challenging quantitative metric

- FWH approach for noise prediction from compressible flow solver



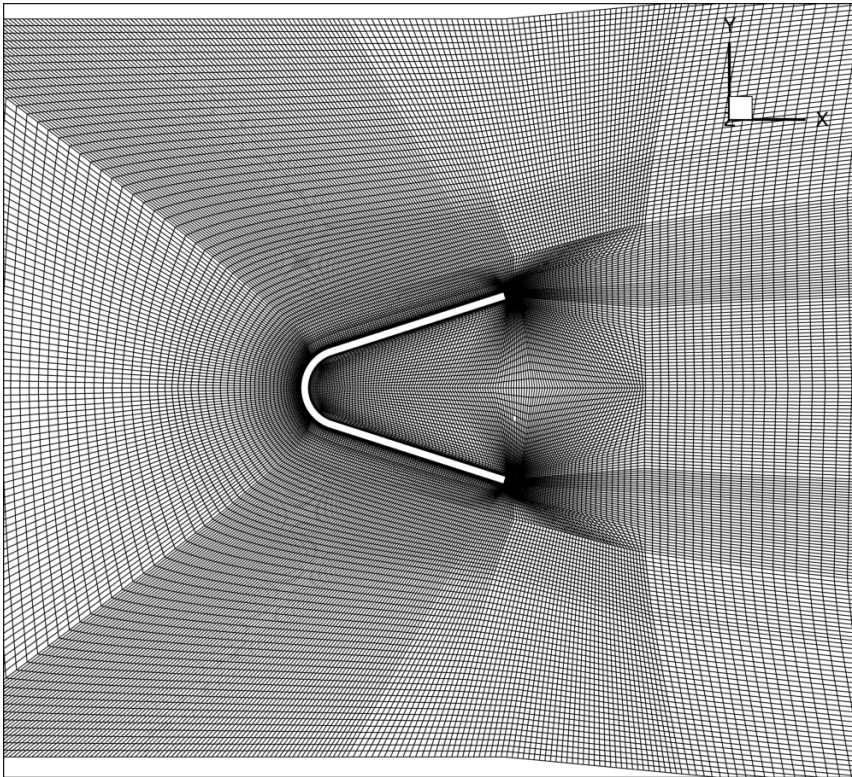
- Reflections from the surfaces outside of the FWH is accounted for using a **method of images**



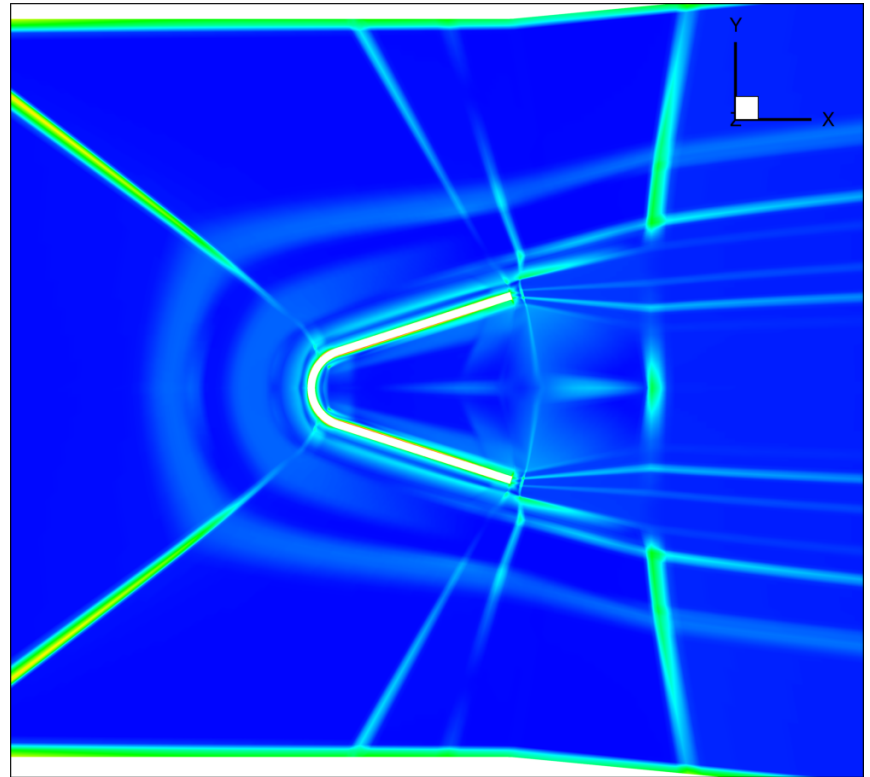
Predicted OASPL : 154 dB
Measured OASPL : 156 dB

Low Dissipation Grid-Sensitive Operators in Charles

- Developed a unstructured mesh quality indicator for turbulent flows based on Summation-By-Parts principles
- E.g. Sub-sonic flow in an augmentor with complex flameholder



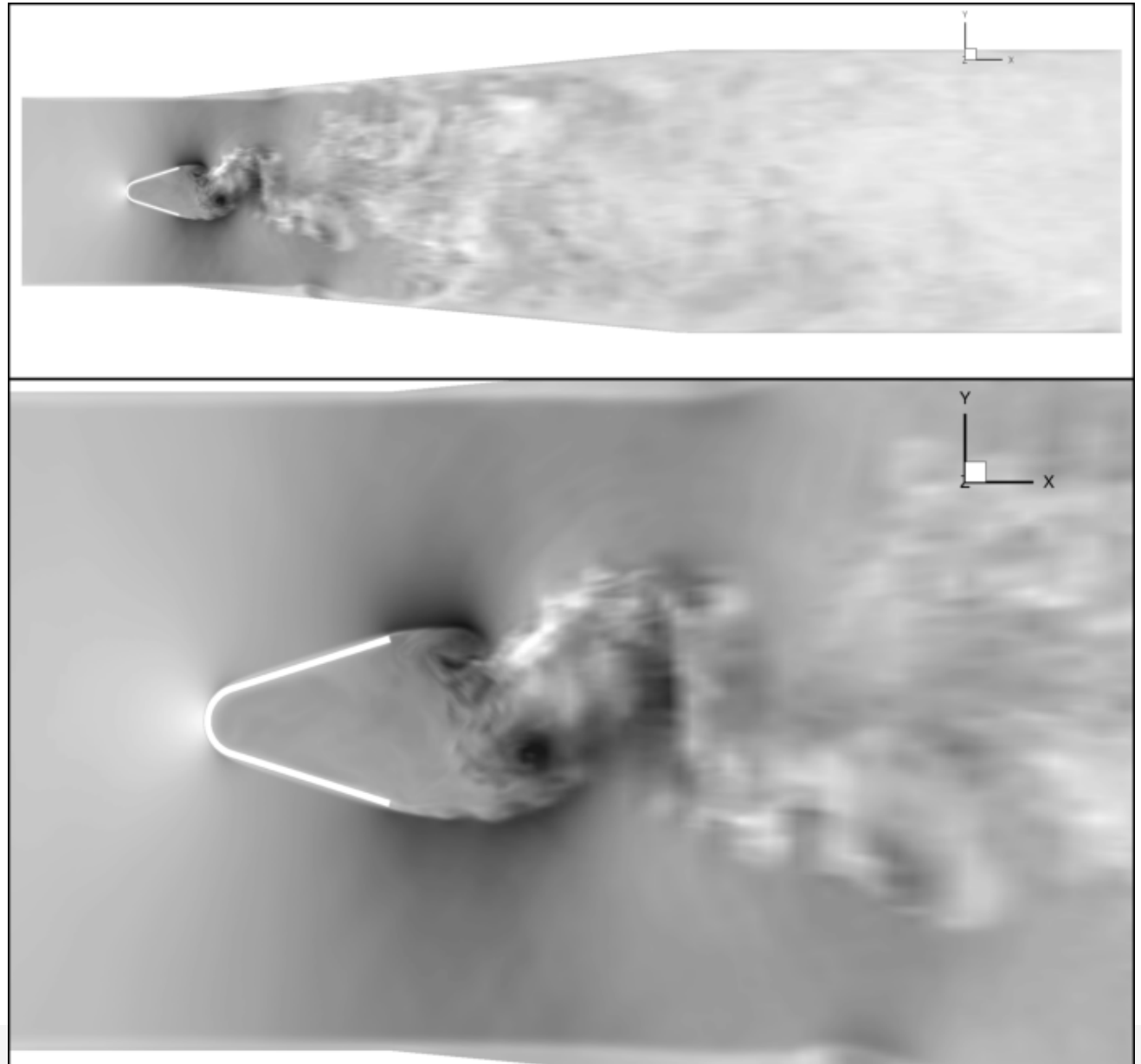
Mesh detail in plane through augmentor flameholder



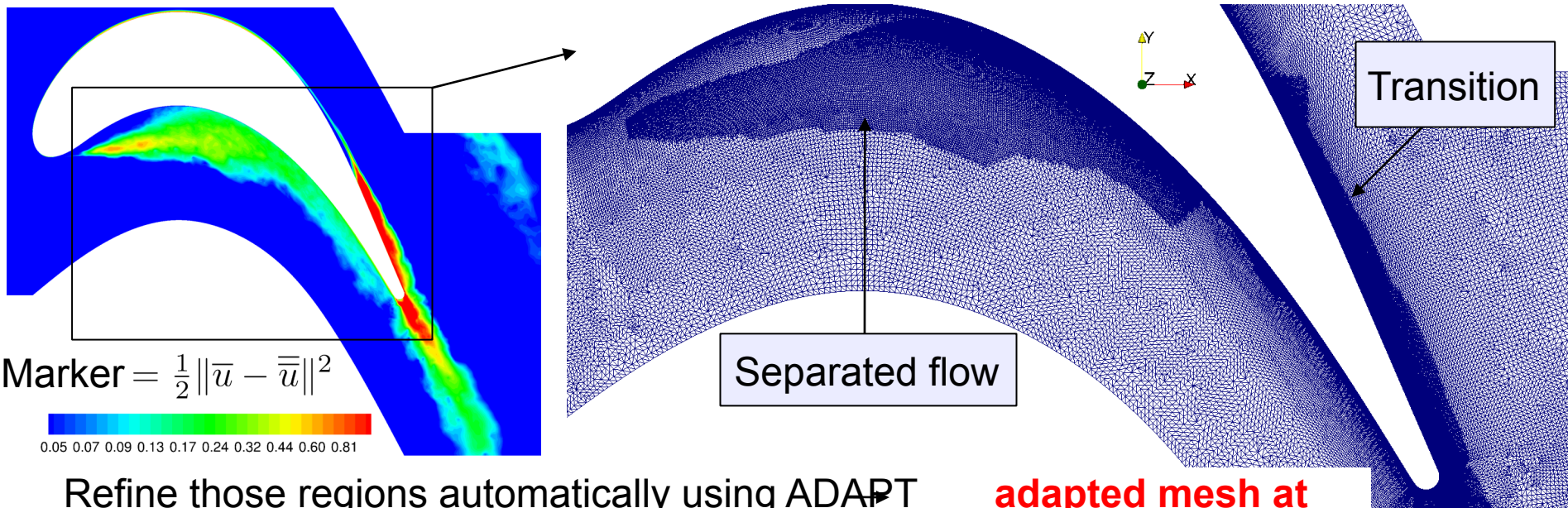
Mesh quality indicator

Non-reacting flow simulation in v-gutter

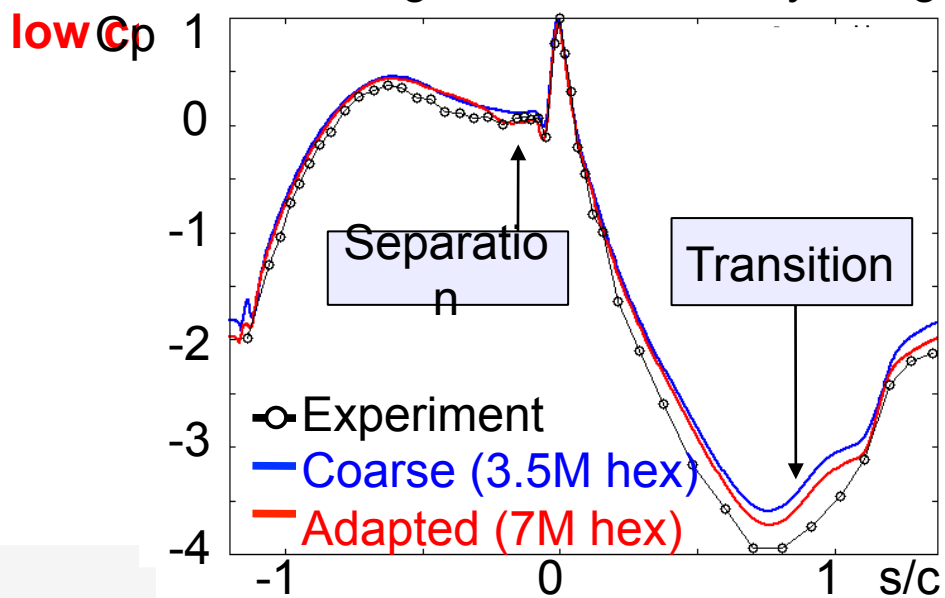
Center plane through
full domain (top) and
detail (bottom)
showing temperature



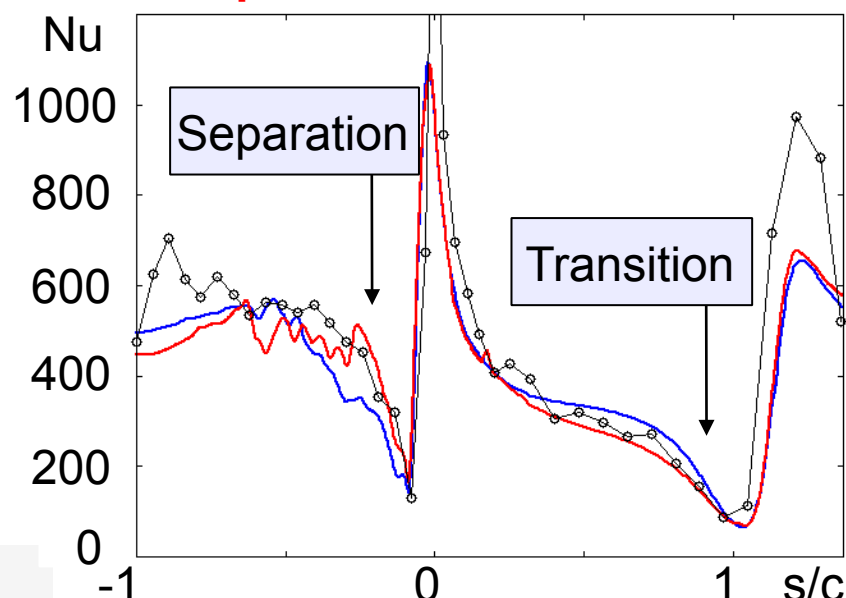
CTR - Summer Program – ADAPT+Cliff



Refine those regions automatically using ADAPT



adapted mesh at



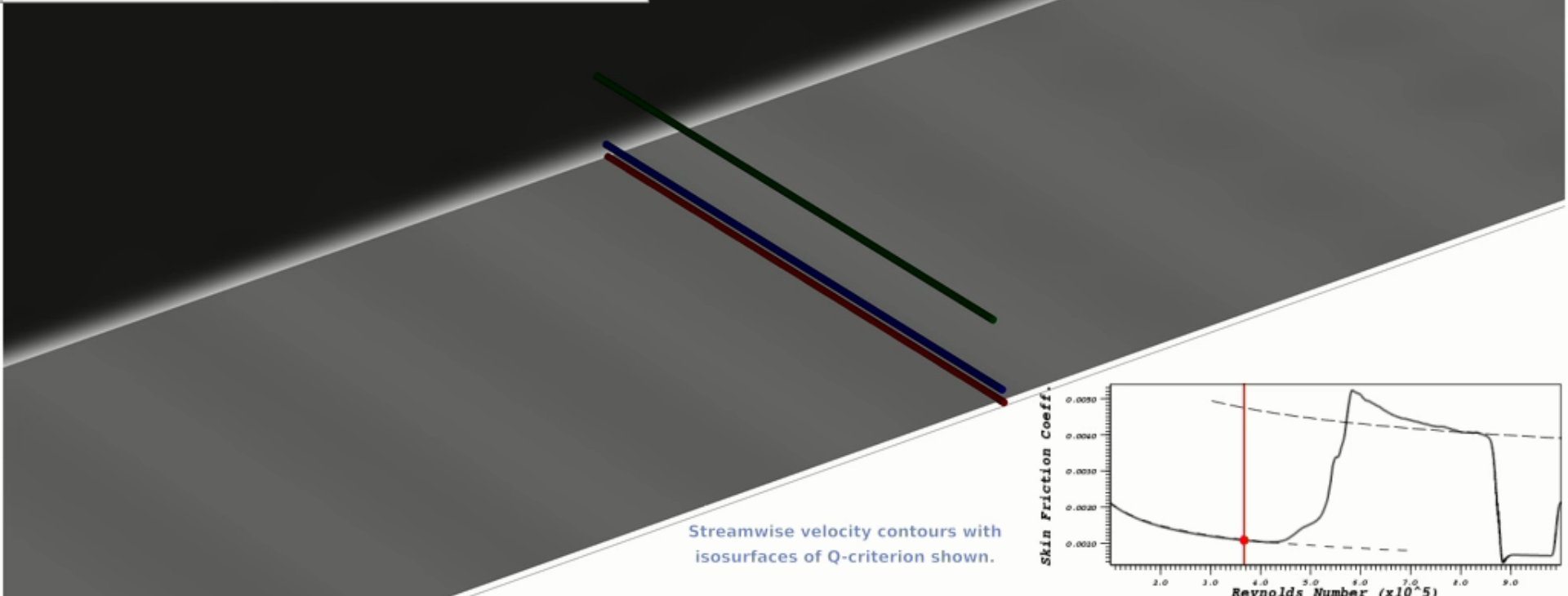
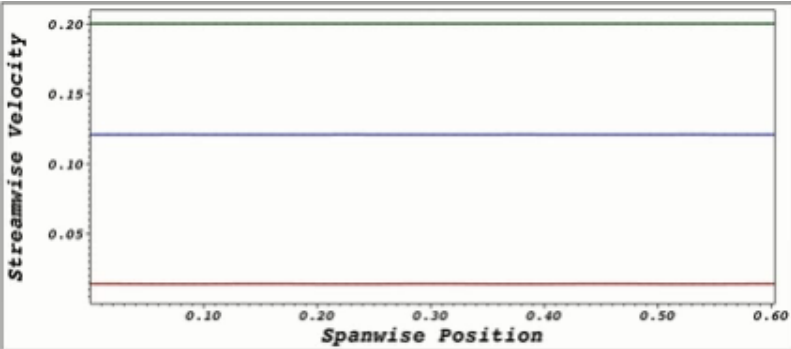
Subgrid scale modeling: The Dynamic Model

- ❑ Model coefficients determined by the local resolved flow, not by user input (eddy viscosity, turbulent Prandtl number, ...)
- ❑ Validation against canonical cases
 - ❑ Rotating flows
 - ❑ Heat transfer in channel
 - ❑ 3D boundary layers
 - ❑ Flow over back step, diffuser (separation)
 - ❑ Flow over cylinder ($Re=3900$)
 - ❑ High Reynolds number mixing layer
 - ❑ Decay of isotropic turbulence
 - ❑ Co-annular jet combustor
 - ❑ Flow over airfoil at angle of attack & control

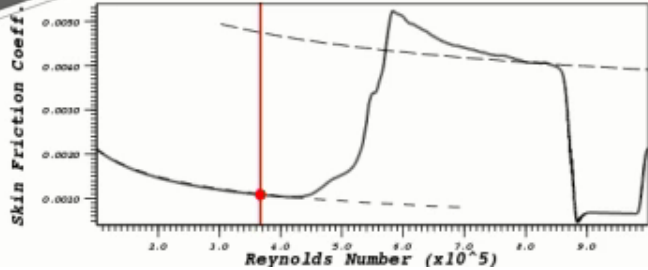
Transition to Turbulence



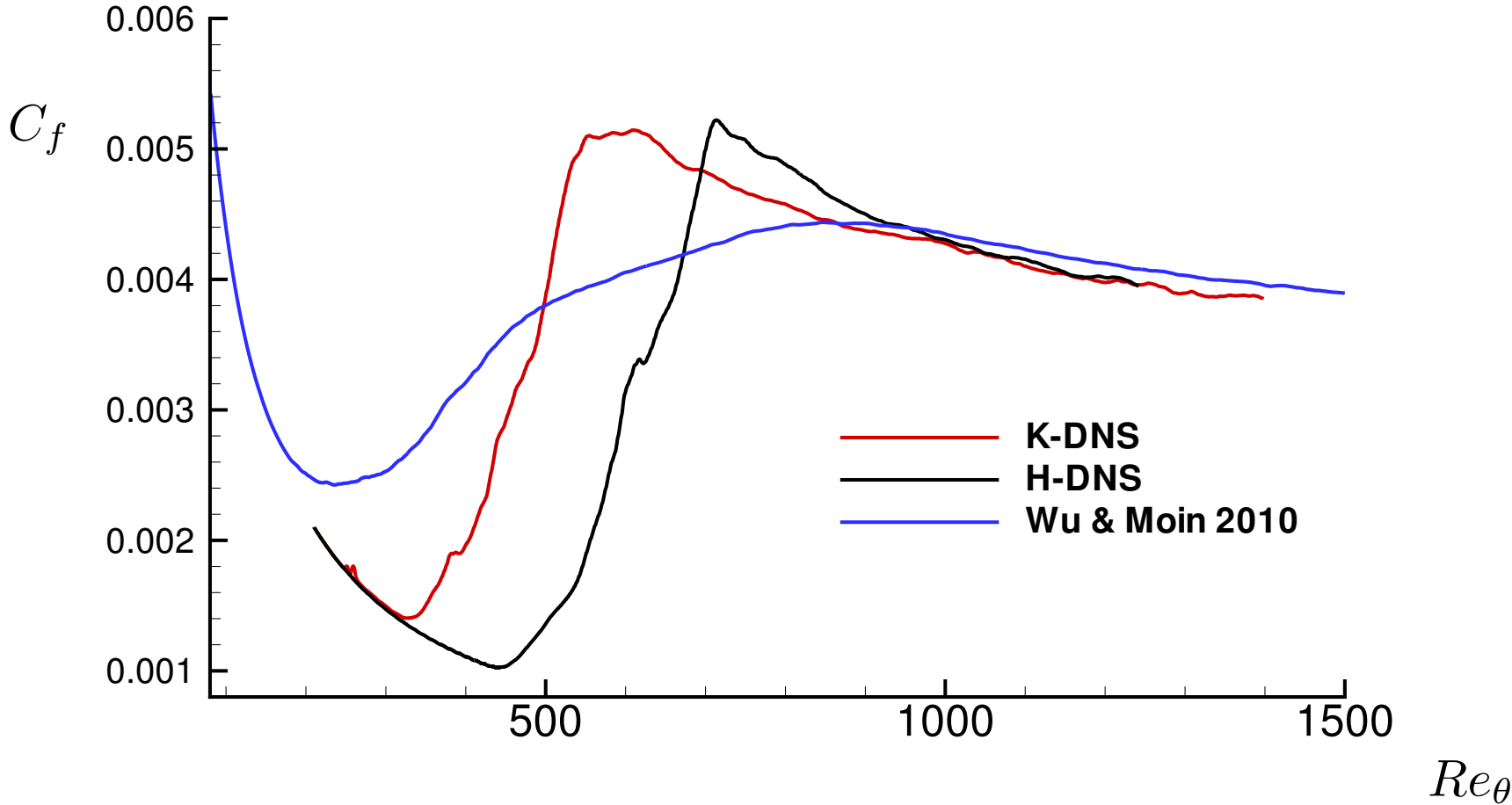
Subharmonic Transition to Turbulence in a
Zero-Pressure Gradient Flat Plate Boundary Layer
Center for Turbulence Research
Stanford University



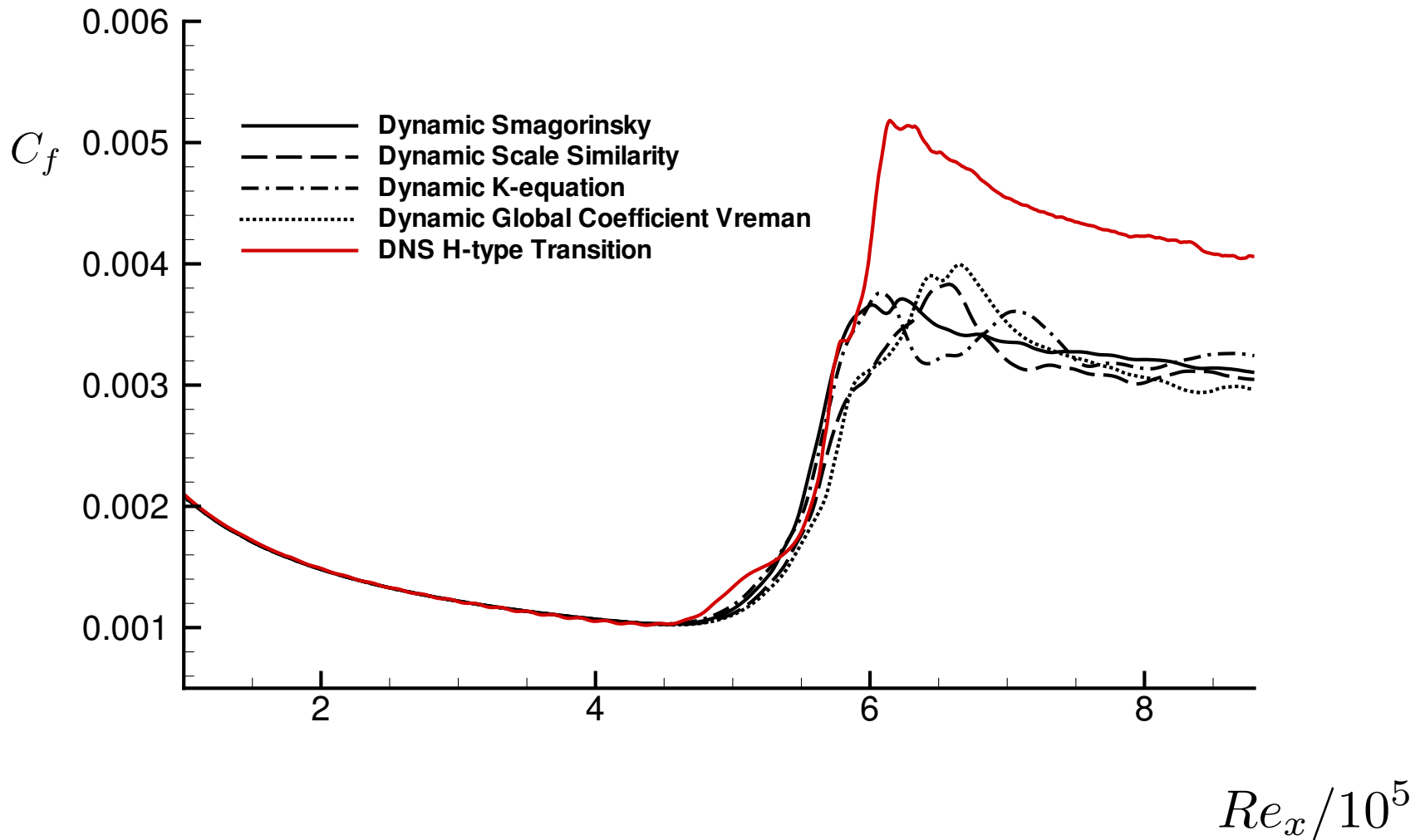
Streamwise velocity contours with isosurfaces of Q-criterion shown.



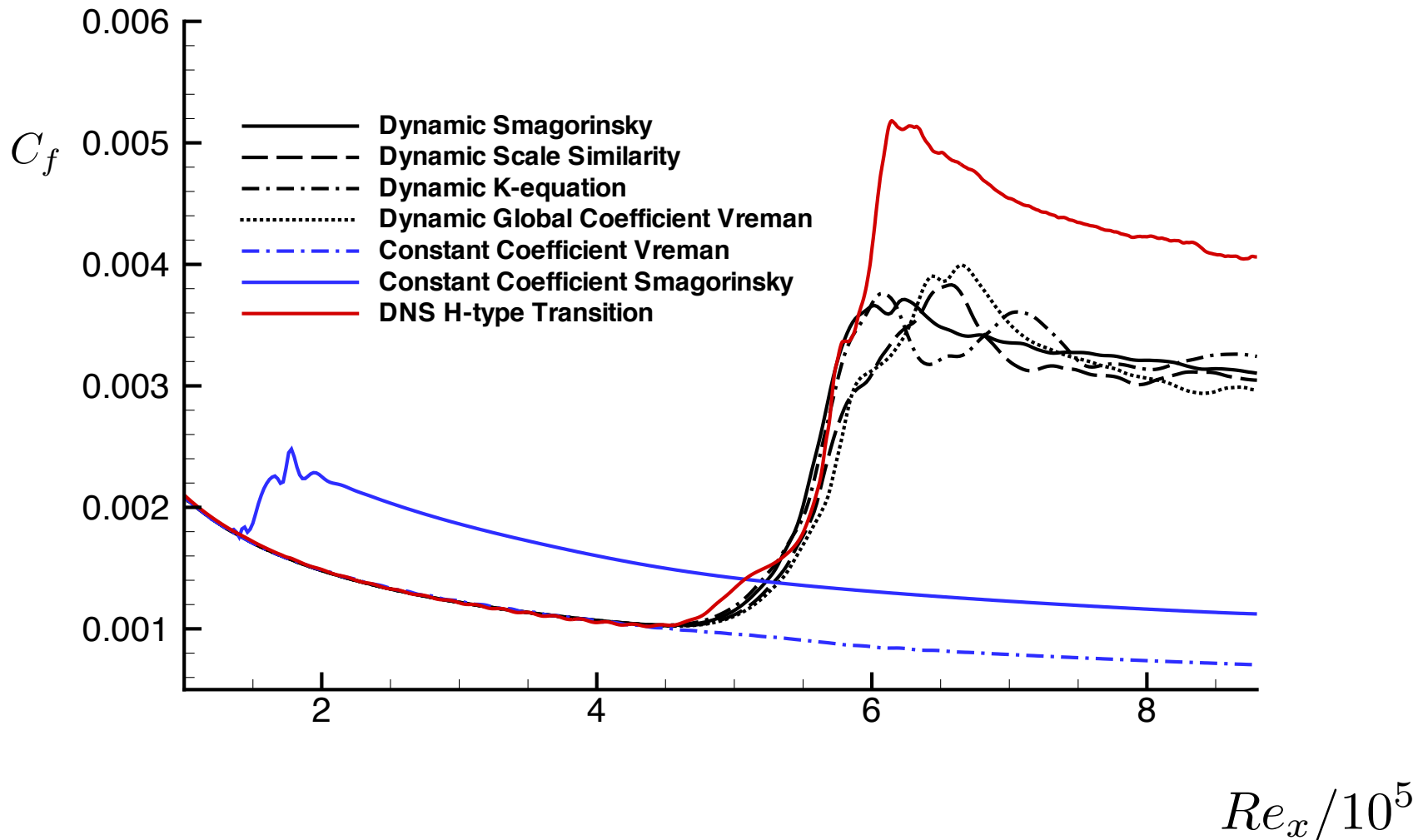
Skin friction coefficient: comparing H-type DNS, K-type DNS and DNS of bypass transition



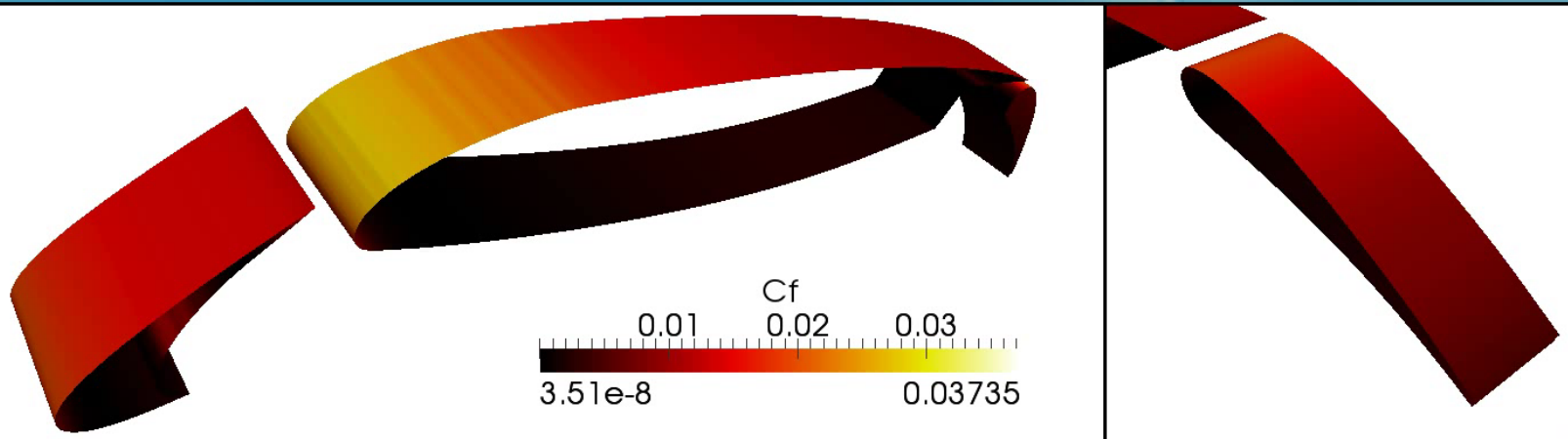
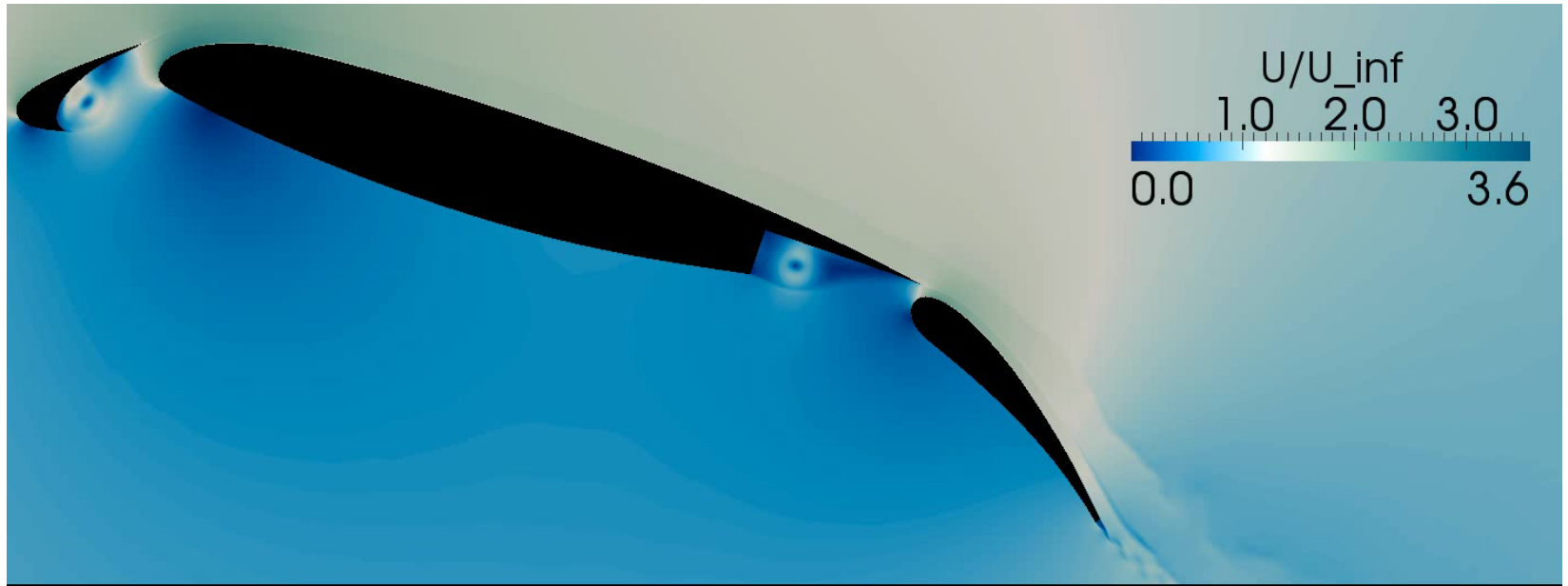
H-type transition: comparing the DNS with dynamic LES models



H-type transition: comparing the DNS to constant coefficient LES models

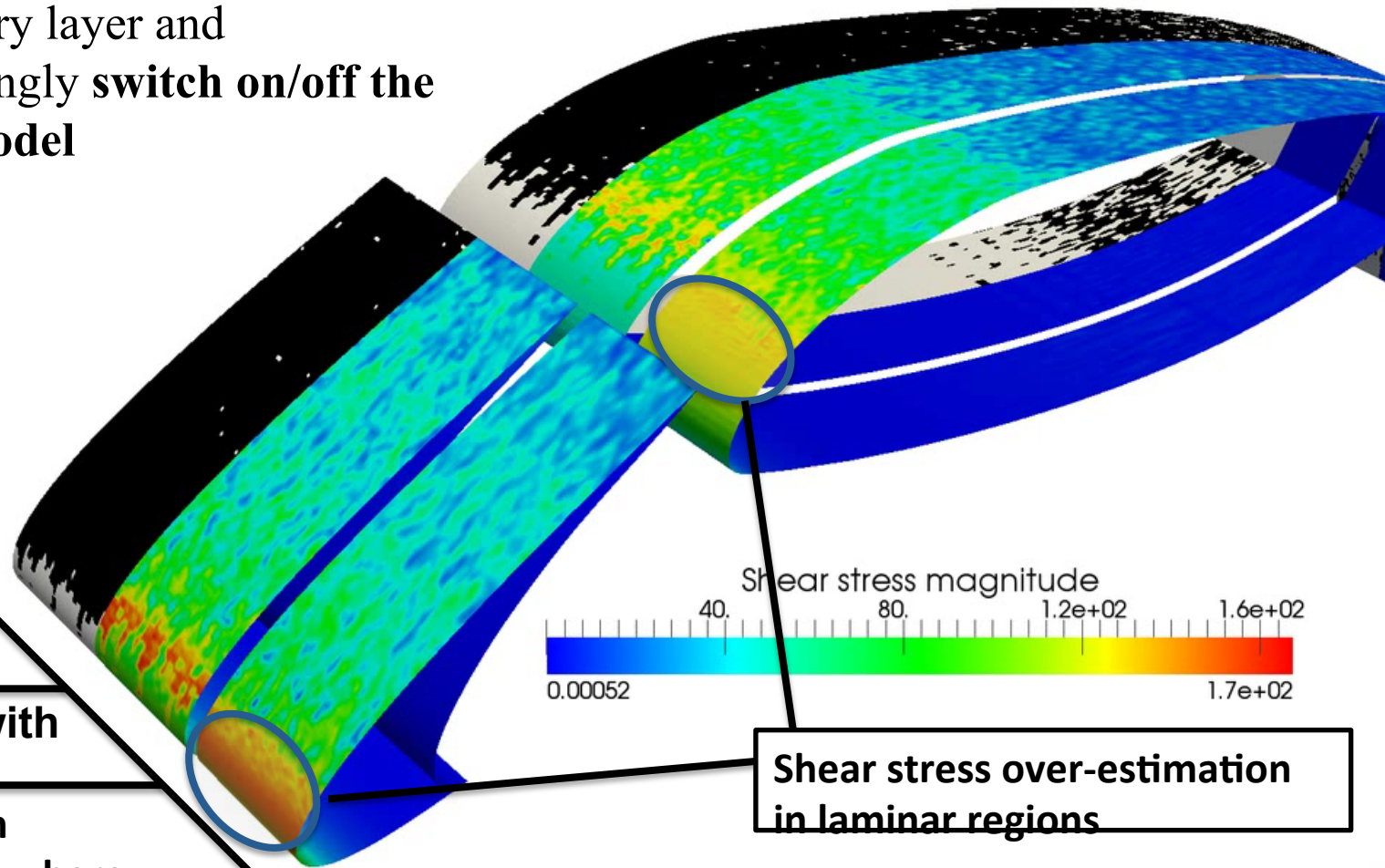


MD 30P30N – Flow field



Dealing with transition and wall-modeling

Our solution: build appropriate and robust sensor to identify the state of the boundary layer and accordingly **switch on/off the wall model**

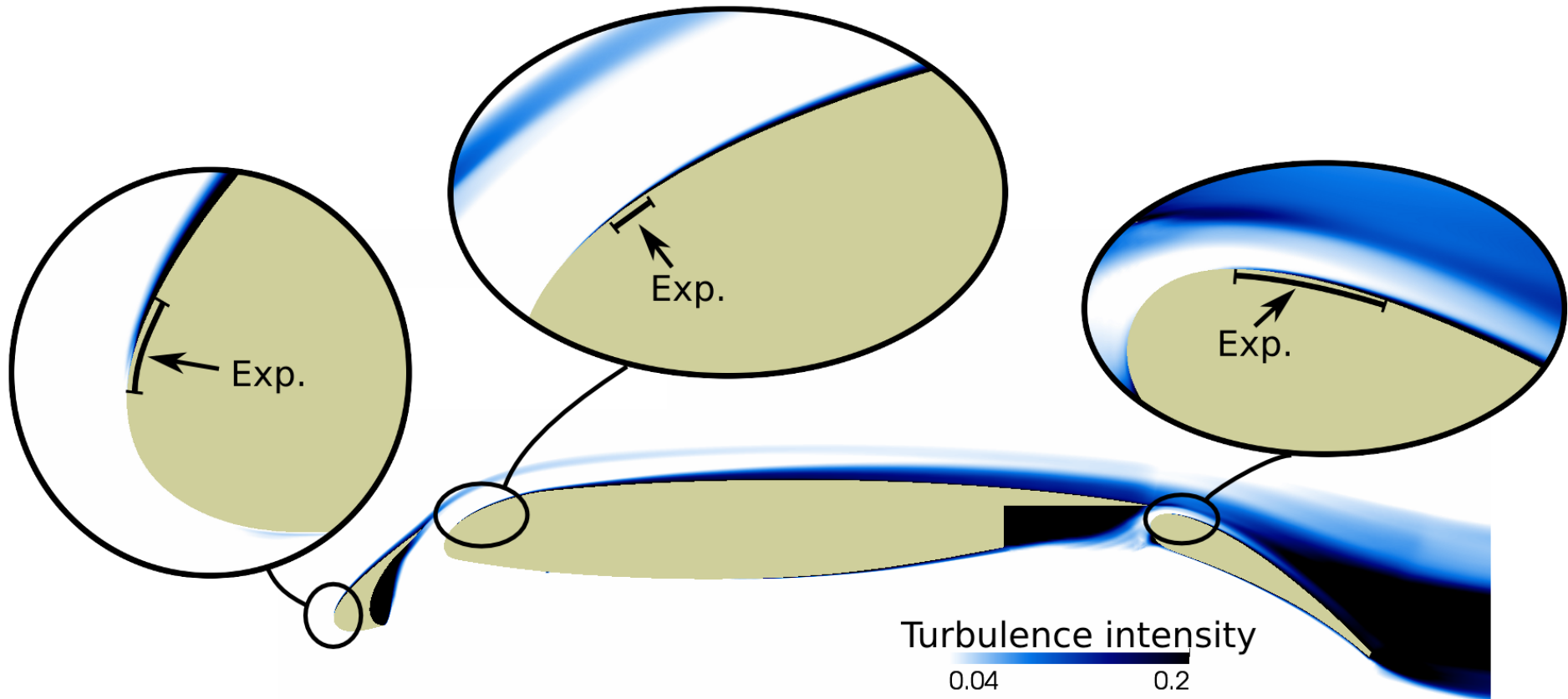


Laminar/Turb.
sensor
Shear stress with
on/off switch
Shear stress with
wall model everywhere

Shear stress over-estimation
in laminar regions

Transition prediction

Comparison with Hot film measurements (A. Bertelrud, *NASA CR*, 1997)



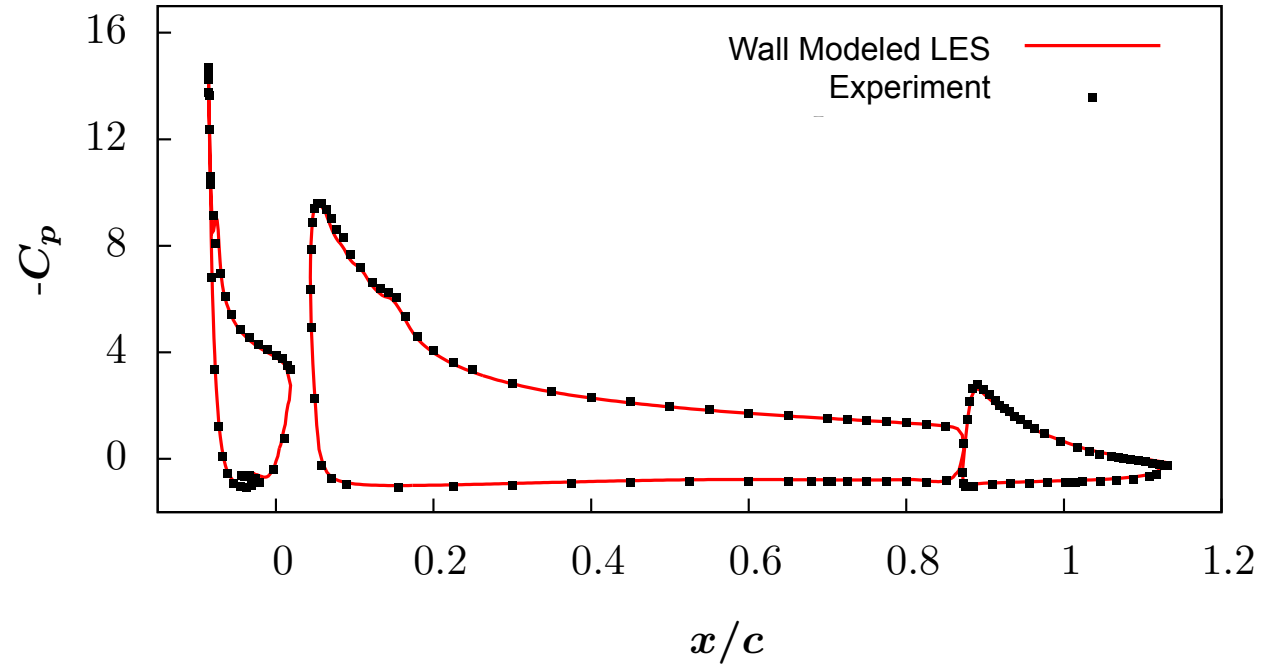
Computed transition location agrees very well with experiments!

MD 30P/30N : aerodynamic coefficient

$$M = 0.2$$

$$Re_c = 9 \cdot 10^6$$

$$\alpha = 19^\circ$$



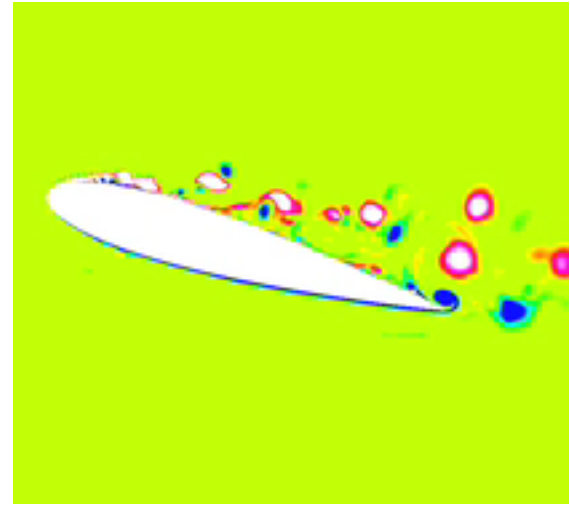
¹ Chin et al (1993)

² Ying et al (1999)

	Lift coefficient				Cost		
	Slat	Main	Flap	Total	Mesh	Steps	CPU Hours
Experiment¹	0.74	3.18	0.36	4.28	-	-	-
Experiment²	0.76	3.22	0.36	4.34	-	-	-
Wall-modeled LES	0.75	3.23	0.37	4.35	8M	500K	50K

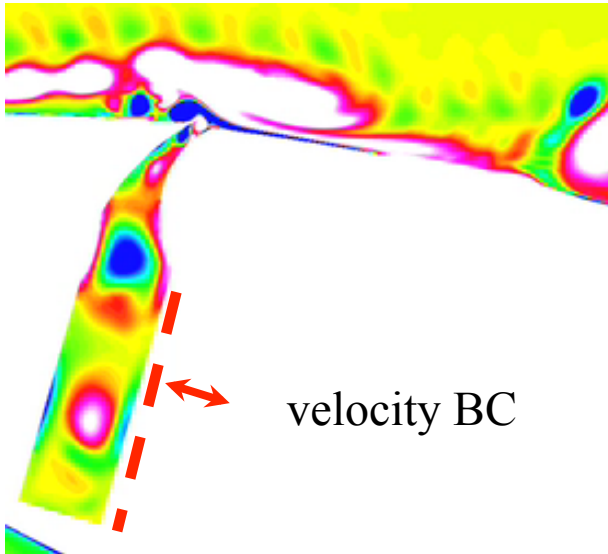
Flow Separation Control: An example of the utility of LES

uncontrolled



$$\Omega_z C / U_\infty = -50 \sim 60$$

synthetic jet actuator



velocity BC

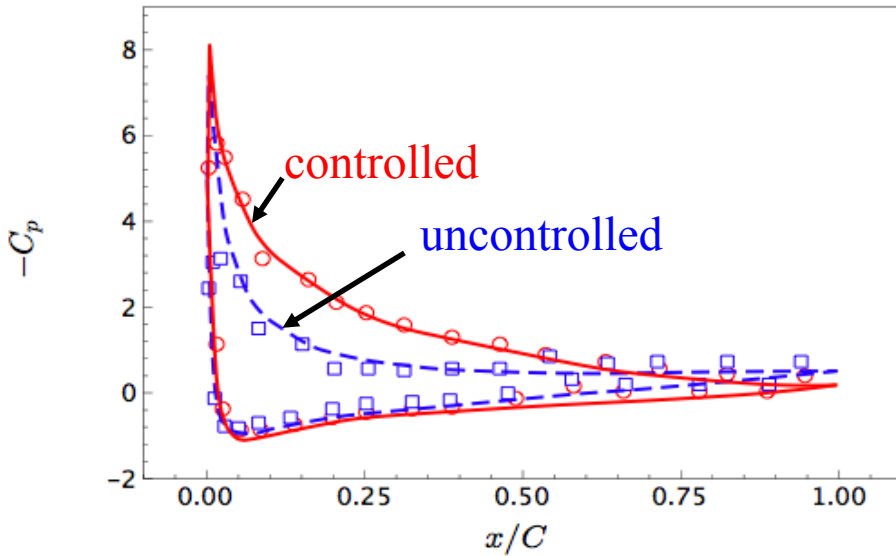
controlled



Flow Separation Control

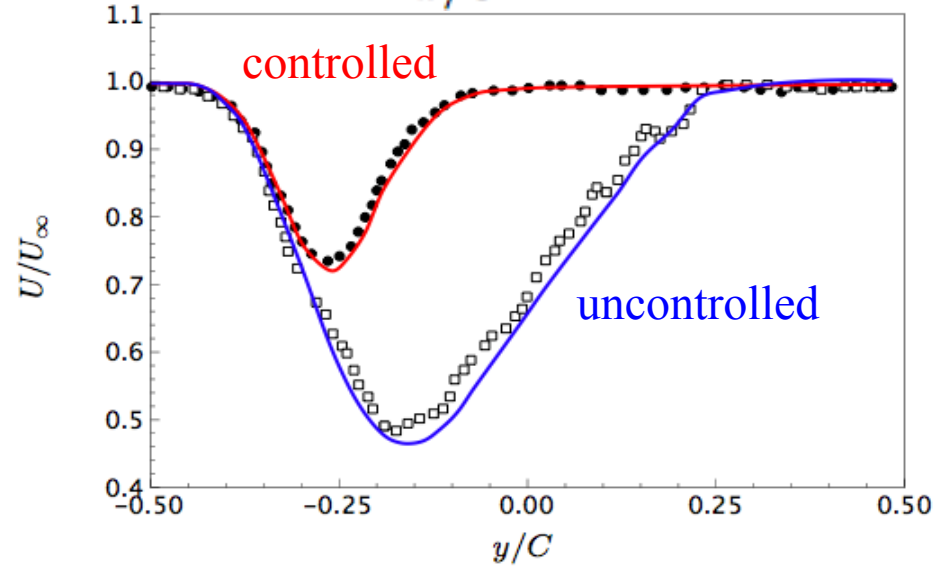
Surface pressure

$$-C_p$$



Velocity in the wake

$$x/C = 1.2$$



Lift coefficient

	Uncontrolled	Controlled
LES	0.83	1.43
EXP	0.82	1.41

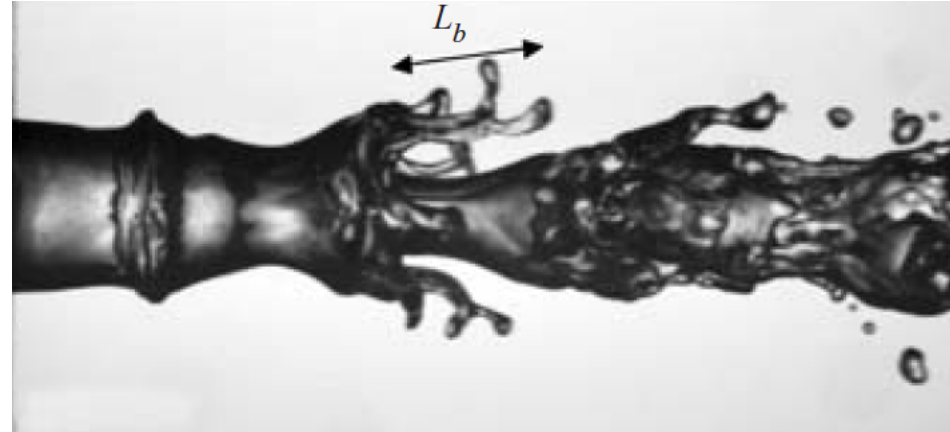
Lines: LES

Symbols: Experiments (Gilarranz *et al.*, *JFE*, '05)

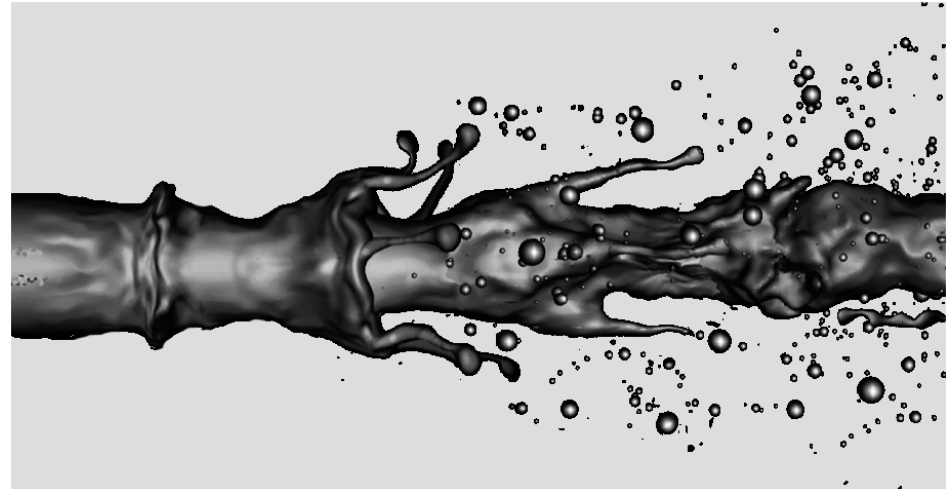
Subgrid scale modeling in two phase flow

- Common practice in CFD to inject distributions of Lagrangian drops to represent fuel spray
- Based heavily on empirical correlations and experimental data – not predictive
- Need to be able to simulate primary atomization of fuel with high-fidelity approaches
- Physics-based subgrid scale models of fuel breakup are required

❑ Experiment (Marmottant et al.)



❑ Numerical Simulation

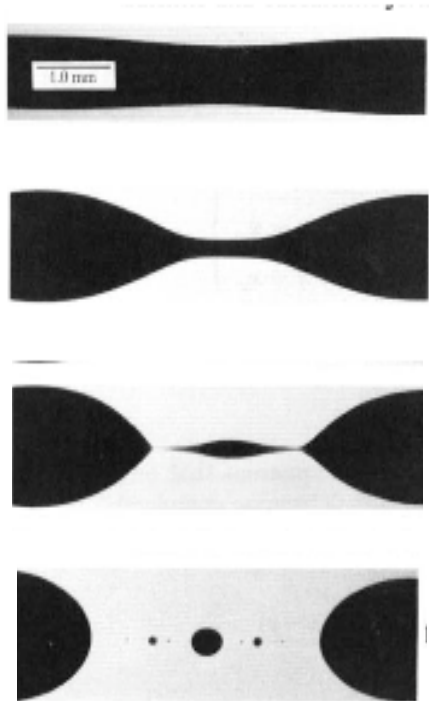


Time = 0.00

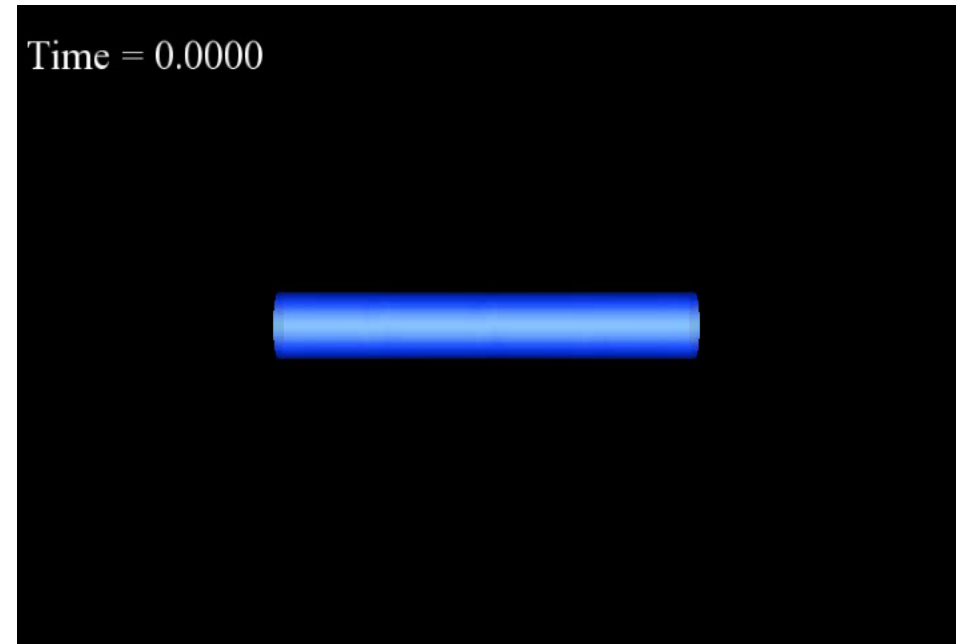


Physical Breakup Process: pinching-off

Experiment (Tjahjadi et al. JFM 1992)



Refined Level set Grid Method (Herrmann 2008)



- Capillary instability leads to formation of satellite drops
- Number and size of drops can be predicted using stability theory

$$\frac{\Delta}{D} = 0.09$$

Physical Breakup Process: pinching-off

Experiment (Marmottant et al.)

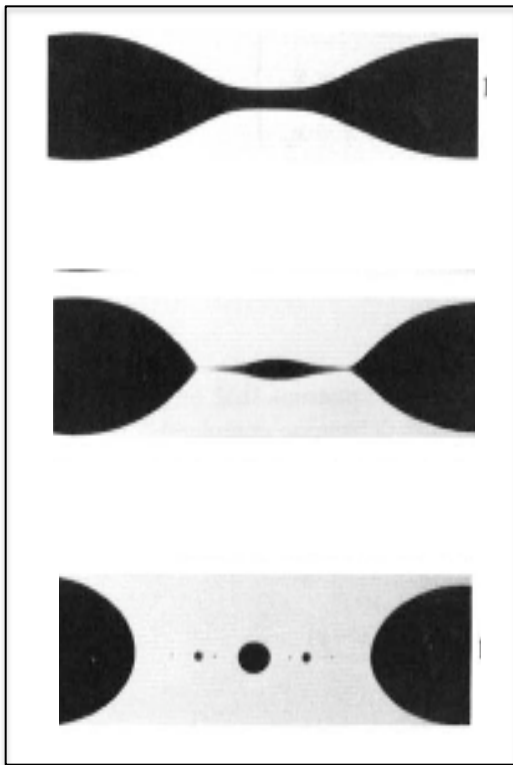


- Ligaments undergo similar instability, pinching off to form small drops

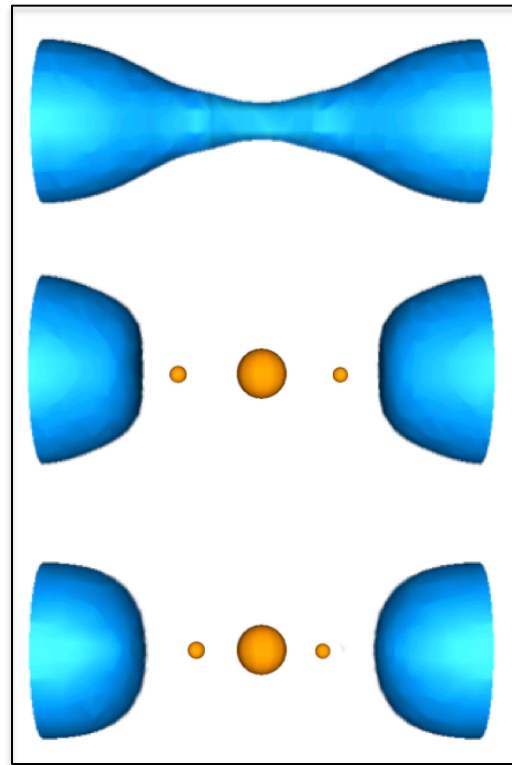
Subgrid scale modeling concept

Method proposed by Kim & Moin (2011):

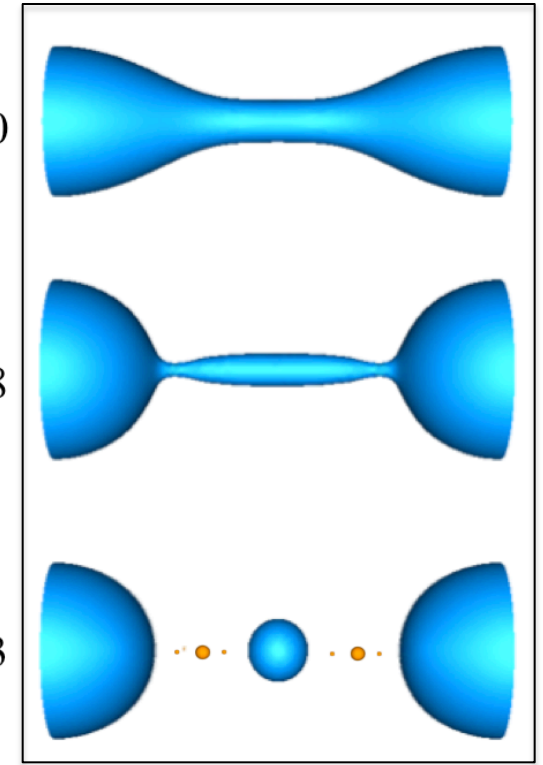
1. Detect ligament using resolution criteria
2. Locally solve stability problem with interface geometry as initial condition
3. Replace ligament with drops in Lagrangian DPM



Experiment



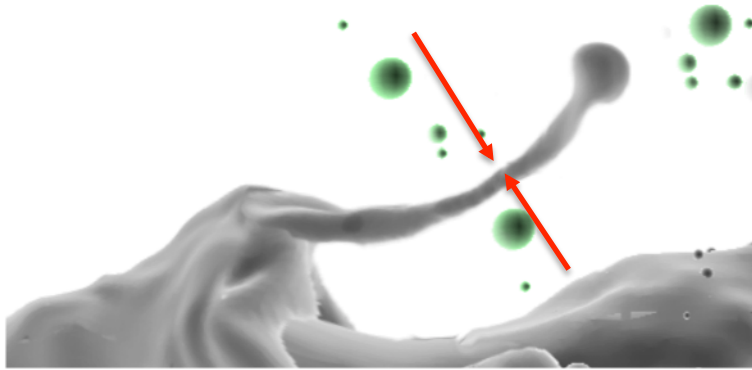
Coarse grid $\frac{\Delta}{D} = 0.18$



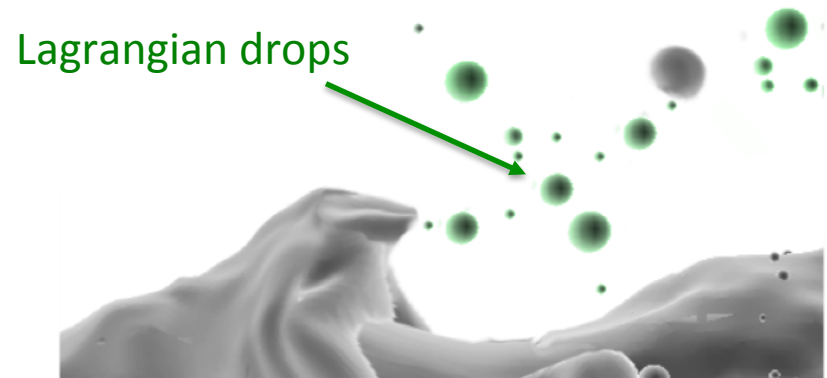
Fine Grid $\frac{\Delta}{D} = 0.09$

Subgrid scale model in action

- Subgrid droplet model in action for the coaxial liquid jet simulation



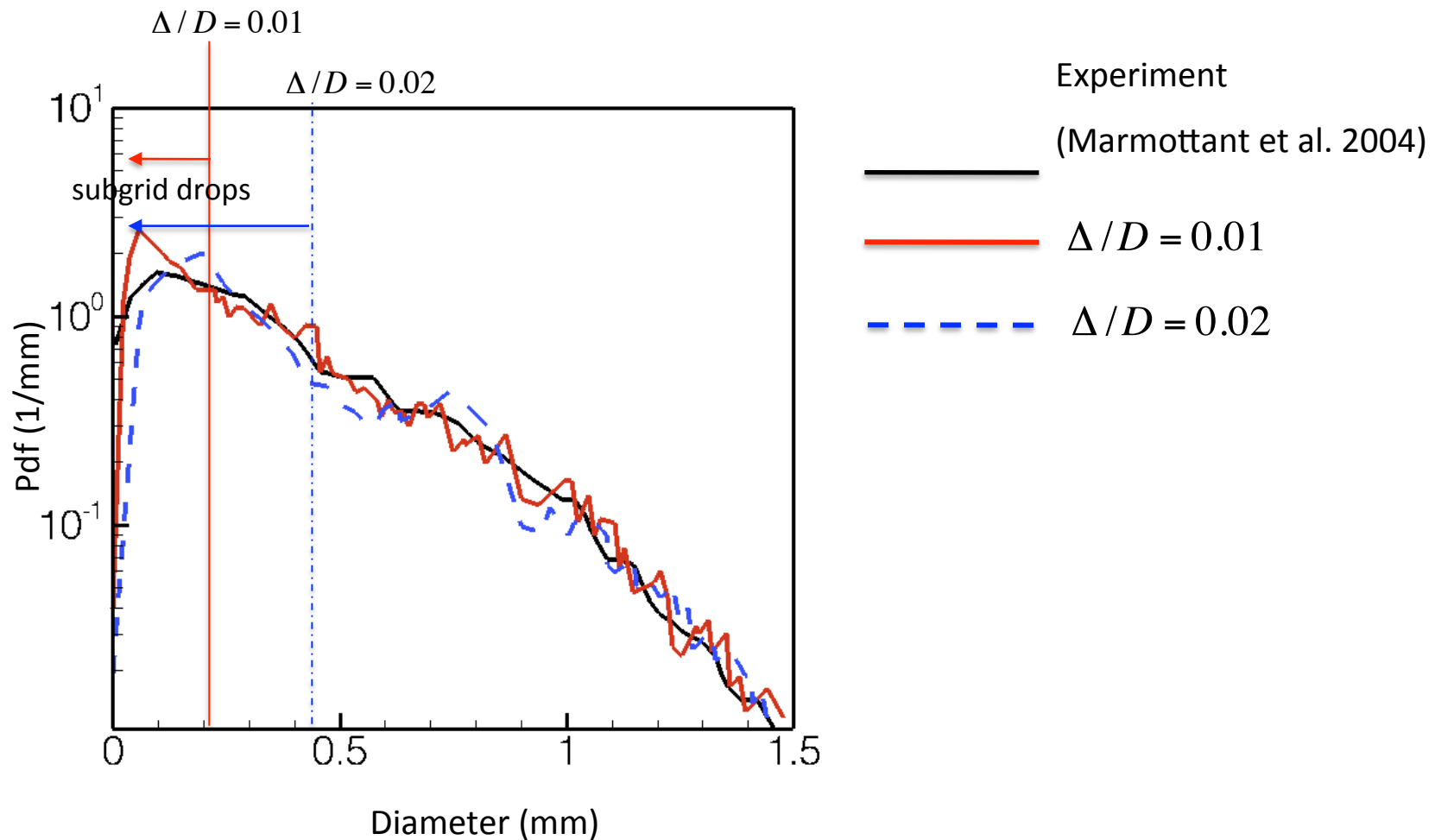
Ligament just above detection threshold



Ligament replaced by satellite drops

Sub-grid scale model validation

- Quantitative comparison to measured droplet pdf



Reacting Flow Challenges

Several competing approaches differing in cost, turbulence closure, complexity of chemical mechanism, combustion regime,

Flamelet/Progress-Variable approach

- Assumes thin flame structure
- Tabulation of complex chemistry -> Reasonable cost
- Must be extended to include complex effects
 - Autoignition, heat transfer, slow species, different regimes

PDF/FDF Transport approaches

- Accurate chemistry and turbulence closure, but costly
- Issues with mixing closure

Reduced Mechanisms

- Turbulence closure problem

Advocate for a balanced approach that doesn't preference chemical fidelity over flow fidelity, geometric fidelity

Building on the FPV Formulation

Heat Transfer

Shunn & Moin, 2007

NOx modeling and Radiation

Ihme & Pitsch, 2008

Soot modeling

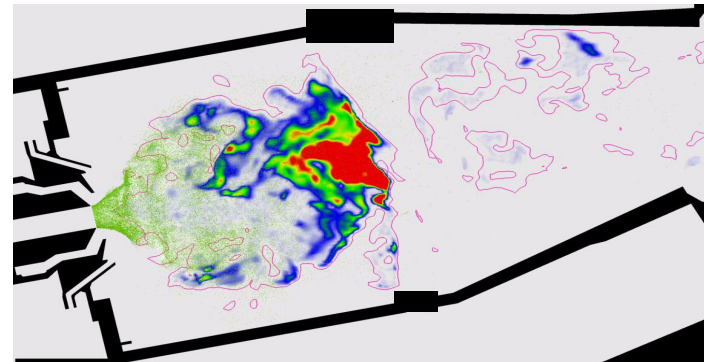
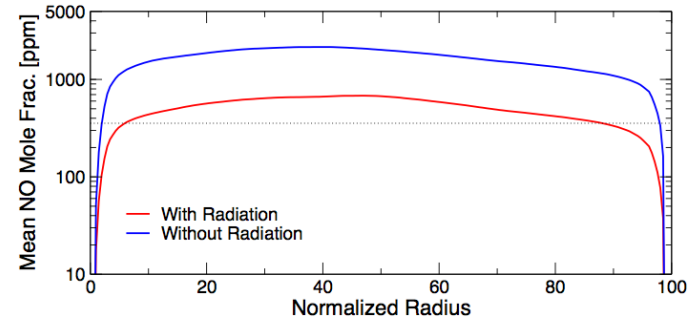
Mueller & Pitsch, 2012

Multi-regime flamelet models

Knudsen & Pitsch, 2009

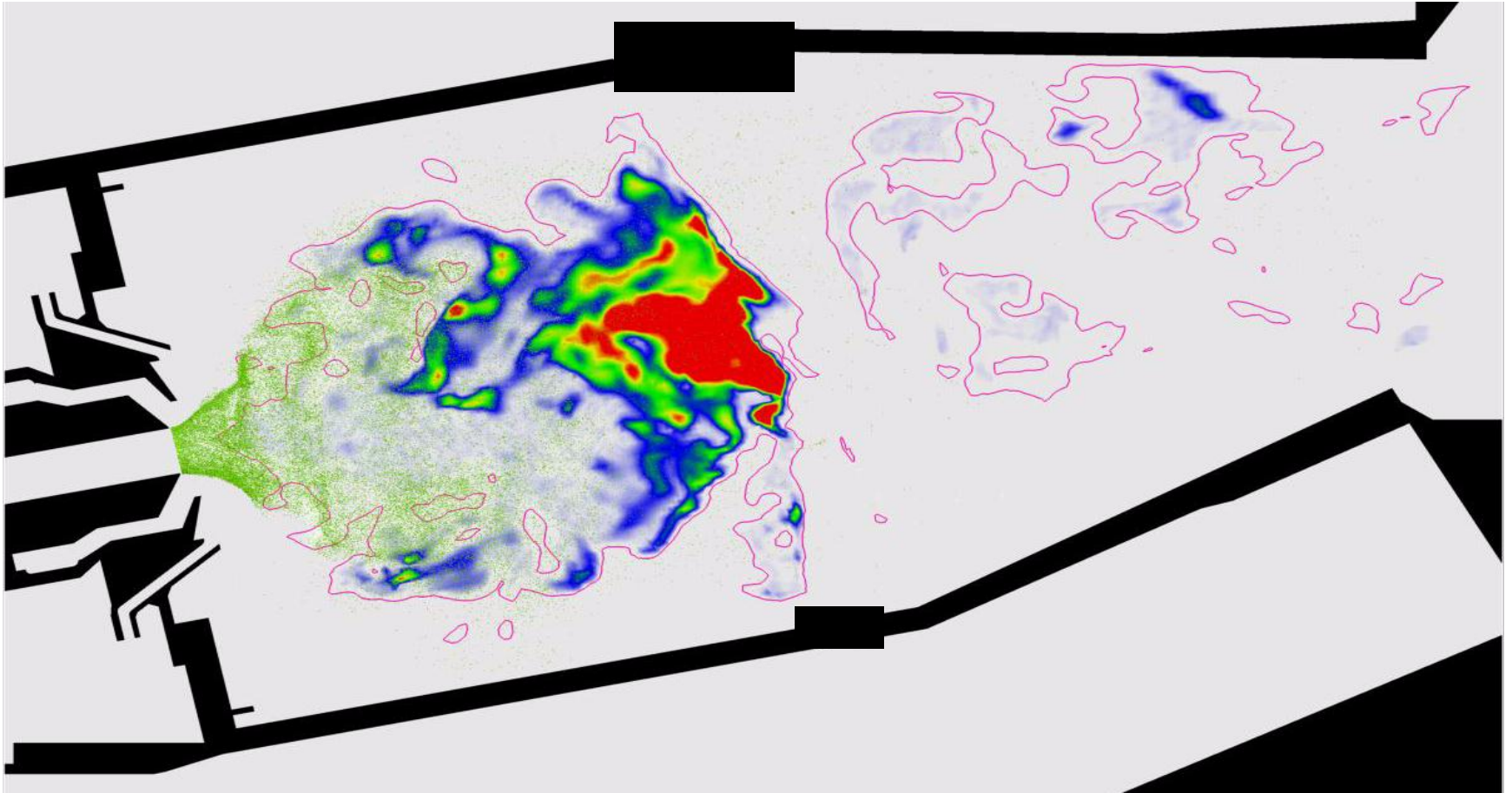
Compressible flamelet formulation

Terrapon et al., 2010



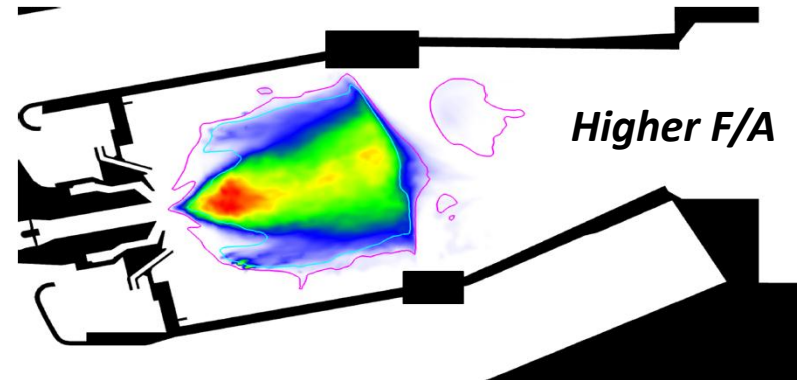
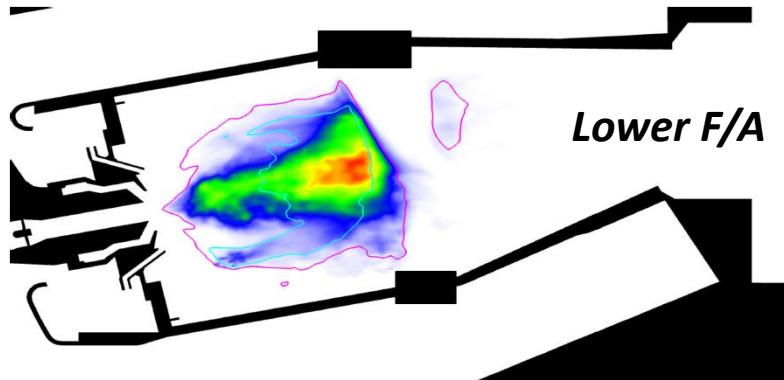
PW6000 Combustor

- Soot Volume Fraction at Lower F/A



PW6000 Combustor

- Soot Volume Fraction



- Comparable volume fractions next to the introduction of dilution air
 - Result of the dominant soot growth mechanism
- At higher F/A, recirculation zone is significantly richer
 - Significant soot volume fraction found in the recirculation zone
 - At lower F/A, recirculation zone mixture fraction is sufficiently small that oxidation is competitive with growth processes
- Downstream near combustor exit, average volume fraction is more than four orders of magnitude smaller than in primary combustion zone

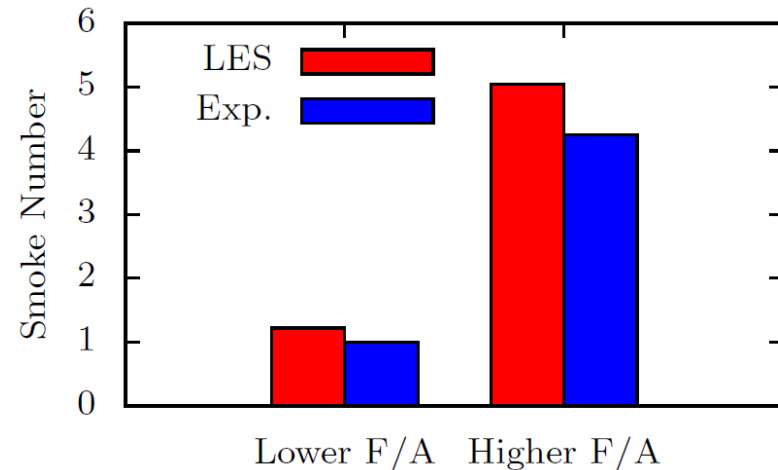
PW6000 Combustor

- Smoke Number Comparisons

- Integral measure of the volume fraction leaving the combustor

Exit Plane Smoke Number¹
(Normalized by Exp. at Lower F/A)

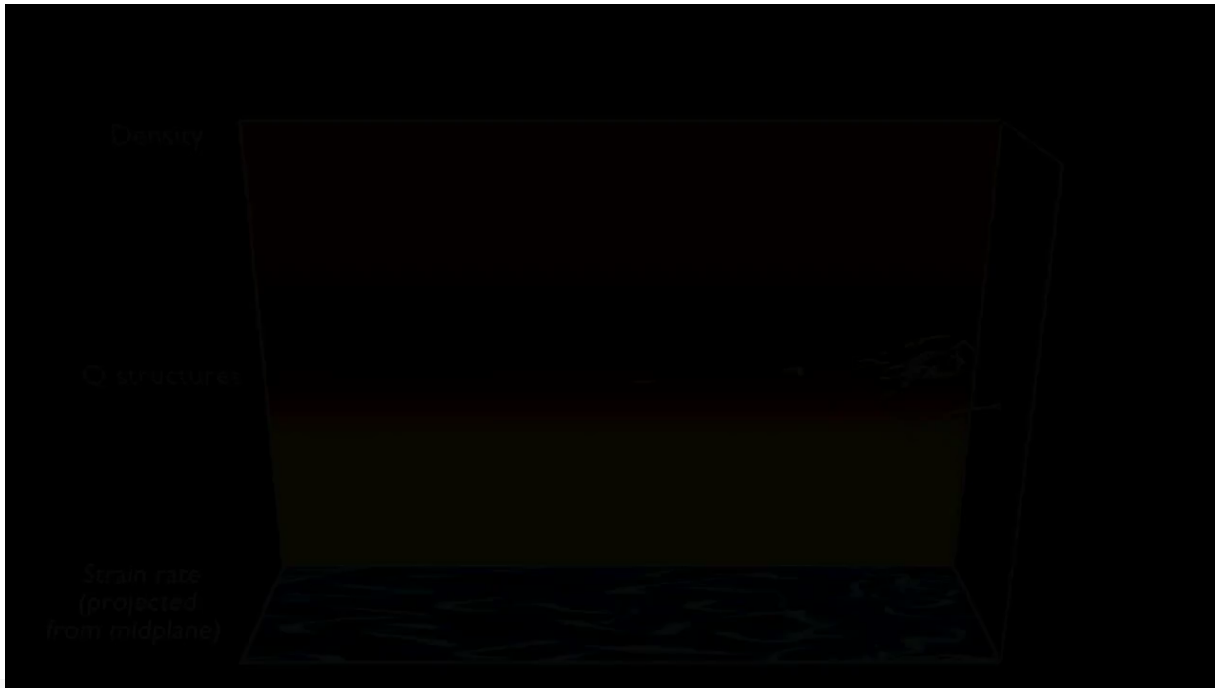
	LES	Exp.
Lower F/A	1.22	1.00
Higher F/A	5.05	4.25
Ratio	4.14	4.25



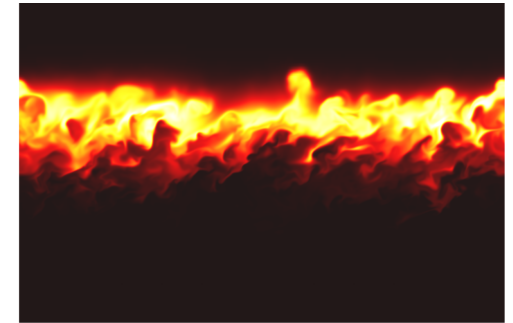
- Reasonable prediction of absolute values; excellent prediction of *quantitative trend*
- Smoke number is very sensitive to the description of radiation
 - Optically thin assumption not appropriate for soot radiation in combustor
 - With soot radiation, local quenching leads to excessive “smoking”
 - Mimic reabsorption by turning off soot radiation

Assessing FPV modeling errors using DNS of Reacting Mixing Layer

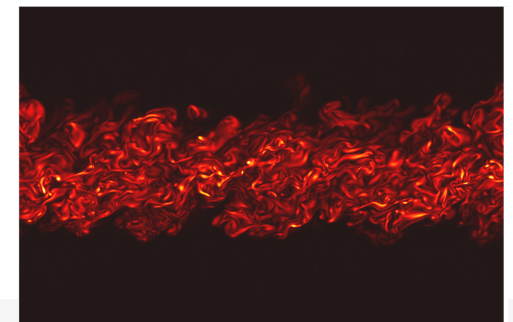
- FPVA is originally developed for low Mach number flows, and has been extended for compressible flows by adding compressibility corrections
- Validate FPVA in supersonic regime using DNS with finite-rate chemistry
- Quantification of epistemic uncertainties in FPVA



OH mass fraction

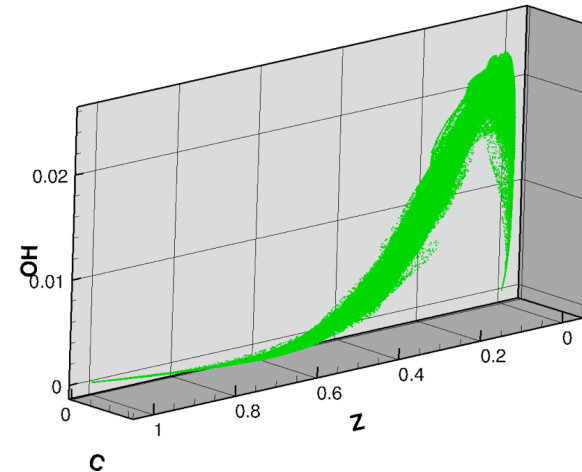


Vorticity magnitude



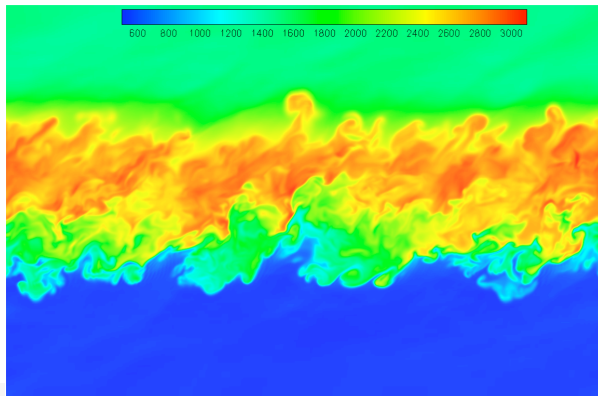
FPVA Validation

- Existence of intrinsic low-dimensional manifolds in supersonic regime

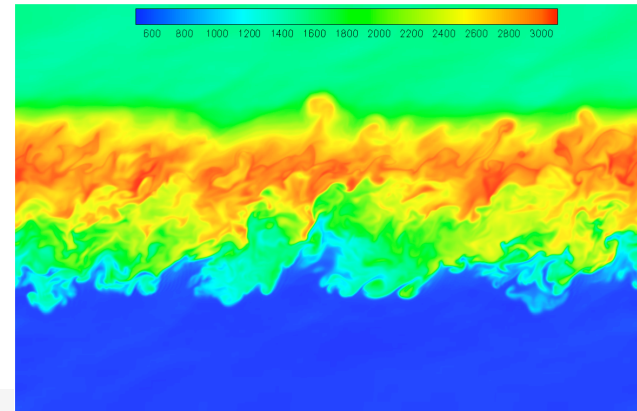


- *A priori* analysis of FPVA

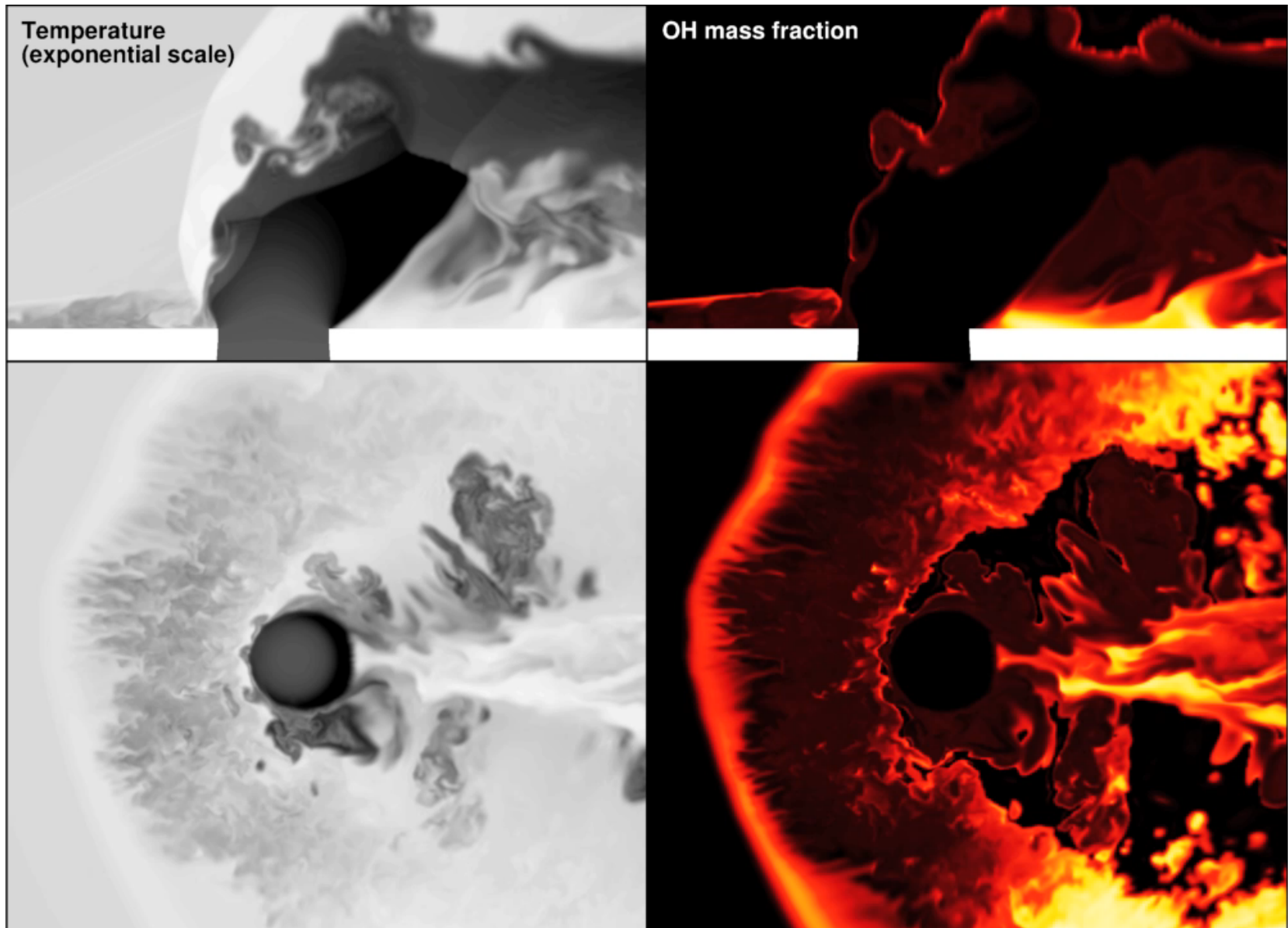
T - DNS



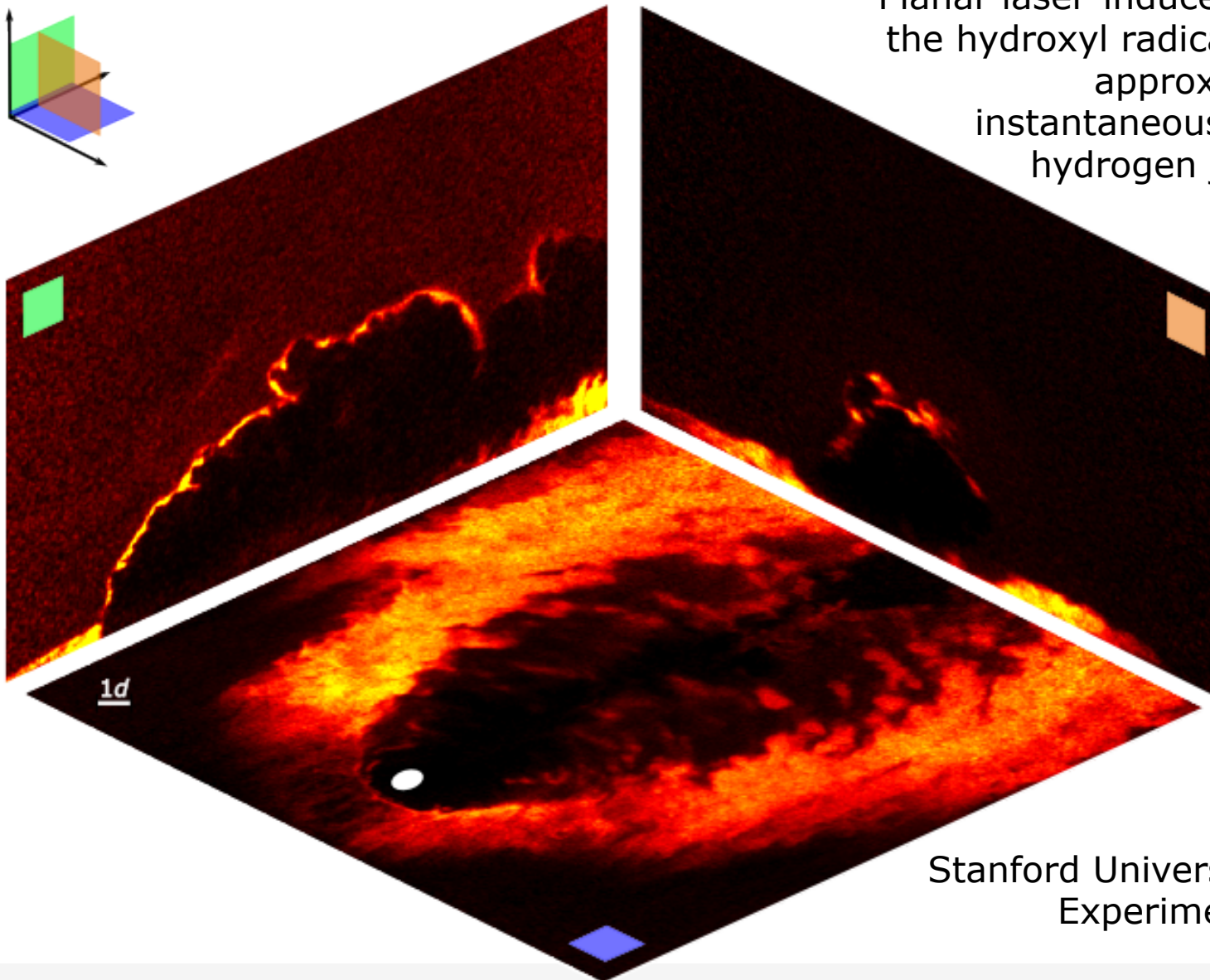
T - FPVA



Reacting Jet in Supersonic Cross-Flow



Strong Interactions with Experimentalists



Planar laser-induced fluorescence of the hydroxyl radical (OH) is used to approximately mark the instantaneous reaction zone of hydrogen jets in supersonic crossflow

Stanford University HTGL
Experiment

Conclusions and Outlook

- Numerical methods and numerical analysis (e.g. stability of multi-physics coupling) remain critical
- Computer power increasing at 100x/7yrs **but** architectures changing rapidly due to power constraints:
 - challenges in programming these heterogeneous systems efficiently (e.g. Liszt DSL)
 - challenges associated with truly massive parallelism: e.g. 1,000,000 cores
- Physics-based subgrid models will remain an important element of LES of multiphysics engineering systems